Theory of linear viscoelasticity of semiflexible rods in dilute solution

V. Shankar, Matteo Pasquali,[a)] and David C. Morse[b)]

Department of Chemical Engineering and Materials Science, University of Minnesota, 421 Washington Avenue, S. E., Minneapolis, Minnesota

Synopsis

We present a theory of the linear viscoelasticity of dilute solutions of freely draining, inextensible, semiflexible rods. The theory is developed expanding the polymer contour about a rigid rod reference state, in a manner that respects the inextensibility of the chain, and is asymptotically exact in the rodlike limit where the polymer length L is much less than its persistence length L_p. In this limit, the relaxation modulus $G(t)$ exhibits three time regimes: At very early times, less than a time $\tau_{\parallel} \propto L^8/L_p^5$ required for the end-to-end length of a chain to relax significantly after a deformation, the average tension induced in each chain and $G(t)$ both decay as $t^{-3/4}$. Over a broad range of intermediate times, $\tau_{\parallel} \ll t \ll \tau_{\perp}$, where $\tau_{\perp} \propto L^4/L_p$ is the longest relaxation time for the transverse bending modes, the end-to-end length decays as $t^{-1/4}$, while the residual tension required to drive this relaxation and $G(t)$ both decay as $t^{-5/4}$. As later times, the stress is dominated by an entropic orientational stress, giving $G(t) \propto e^{-t/\tau_{\text{rod}}}$, where $\tau_{\text{rod}} \propto L^3$ is a rotational diffusion time, as for rigid rods. Predictions for $G(t)$ and $G^*(\omega)$ are in excellent agreement with the results of Brownian dynamics simulations of discretized free draining semiflexible rods for lengths up to $L = L_p$, and with linear viscoelastic data for dilute solutions of poly-γ-benzyl-L-glutamate with $L \sim L_p$. © *2002 The Society of Rheology.*
[DOI: 10.1122/1.1501927]

I. INTRODUCTION

While the theoretical problem of predicting linear viscoelastic functions of dilute polymer solutions was largely solved in the 1950s for the cases of completely flexible (Gaussian) polymers and rigid rods, the corresponding problem for the wormlike chain model has resisted solution. Here, we present a solution to this problem in the relatively simple limit of rodlike chains, of length L much less than their persistence length L_p. The theory is asymptotically exact in the limit $L \ll L_p$, and is found (by comparison to both simulations and experiment) to remain surprisingly accurate for chains of length up to $L \sim L_p$.

The wormlike chain (WLC) model describes the backbone of a polymer as a smooth contour with a finite elastic resistance to bending, but an infinite resistance to tangential extension or compression. Solving this model has proved difficult largely because the dynamical equations for a single such chain are nonlinear, even in the absence of hydrodynamic interactions. The nonlinearity is a result of the constraint of inextensibility,

---

[a)]Present address: Department of Chemical Engineering, Rice University, 6100 Main St., Houston, TX 77005.
[b)]Author to whom correspondence should be addressed; electronic mail: morse@cems.umn.edu

which must be enforced by a tension (i.e., Lagrange multiplier) field whose value at each point on a chain depends upon the conformation of the entire chain. The physical reason for treating such polymers as inextensible is suggested by a simple model of a wormlike chain as cylindrical elastic solid of diameter a and Young's modulus Y: The energy per unit length required to change the length of such a cylinder by a specified fractional strain is proportional to Ya^2, while the energy per length required to bend it into an arc of radius R is of order Ya^4/R^2, which is smaller than the strain energy by a factor of order $(a/R)^2$. This property of thin, weakly curved filaments is familiar to anyone who has tried to bend and stretch a thread or human hair.

An influential previous theory for the viscoelasticity of solutions of wormlike chains [Harris and Hearst (1966); Hearst *et al.* (1966)] attempted to bypass the difficulties posed by the inextensibility constraint by introducing a modified Gaussian model in which the constraint is imposed only in a temporally and spatially average sense, by a constant Lagrange multiplier tension. This and related Gaussian models yield reasonable approximations for many static properties, and some dynamic properties, but, we find, yield qualitatively incorrect results for the viscoelasticity of solutions of semiflexible rods, because they neglect flow-induced constraint forces. We find that, at all frequencies for which the behavior of semiflexible rods in solution differs substantially from that of true rigid rods, the polymeric contributions to the stress is dominated by contributions arising from constraint forces, and that a rigorous treatment of the constraint is thus a necessity.

The absence of an adequate theory has not prevented the accumulation of a body of experimental data on the viscoelasticity of dilute solutions of wormlike polymers, much of it by J. Schrag and coworkers [Warren *et al.* (1973), Nemoto *et al.* (1975), Carriere *et al.* (1985), (1993)]. Of particular relevance to the present work are measurements of the linear viscoelasticity of dilute solutions of poly(γ-benzyl-L-glutamate) (PBLG) with $L \sim L_p$ by Warren *et al.* (1973) and of somewhat shorter chains, at significantly higher frequencies by Ookubo *et al.* (1976). The measurements of Warren *et al.* revealed that the rigid rod theory of Kirkwood and Auer (1951) adequately describes the behavior of $G^*(\omega)$ for such chains in the low frequency terminal regime, but not at any higher frequencies. The present paper thus focuses on explaining the viscoelasticity of solutions of semiflexible rods at relatively high frequencies, where their behavior differs qualitatively from that of truly rigid rods.

A. Model

We consider a dilute solution of monodisperse wormlike polymers of contour length L, diameter d, and number density c. The conformation of a single chain is parametrized by a space curve $\mathbf{r}(s)$, where s is the arc length measured along the contour of the polymer. The bending energy of a wormlike chain with a bending rigidity κ is given by

$$U_{\text{bend}} = \frac{1}{2}\kappa \int_0^L ds \left| \frac{\partial \mathbf{u}(s)}{\partial s} \right|^2, \tag{1}$$

where $\mathbf{u}(s) \equiv \partial \mathbf{r}(s)/\partial s$ is the local tangent vector, and $\partial \mathbf{u}(s)/\partial s$ is a curvature vector, whose magnitude is the inverse of the local radius of curvature. The constraint of local inextensibility is expressed as a requirement that $|\partial \mathbf{r}(s)/\partial s| = 1$ at each point on the chain, so that $\mathbf{u}(s)$ is a unit vector. The persistence length $L_p \equiv \kappa/k_BT$ is the distance along the chain over which tangent vectors remain correlated in equilibrium. Chains with $L \gg L_p$ thus are (globally) random coils, whereas those with $L \ll L_p$ are semiflexible rods.

The Brownian motion of a single free-draining wormlike chain in an imposed mean flow with velocity gradient $\dot{\boldsymbol{\gamma}} \equiv (\boldsymbol{\nabla}\mathbf{v})^T$ is described by the Langevin equation

$$\boldsymbol{\zeta}\cdot\left(\frac{\partial\mathbf{r}}{\partial t} - \dot{\boldsymbol{\gamma}}\cdot\mathbf{r}\right) = -\kappa\frac{\partial^4\mathbf{r}}{\partial s^4} + \frac{\partial}{\partial s}\left(\mathcal{T}\frac{\partial\mathbf{r}}{\partial s}\right) + \boldsymbol{\eta}. \tag{2}$$

Here, $\boldsymbol{\zeta}$ is a local friction tensor of the form $\boldsymbol{\zeta} = \zeta_\parallel\mathbf{uu} + \zeta_\perp(\mathbf{I}-\mathbf{uu})$ where $\zeta_\parallel$ and $\zeta_\perp$ are friction coefficients for motions parallel and perpendicular to the local tangent $\mathbf{u}(s)$, respectively. The left side of Eq. (2) is a hydrodynamic frictional force. The first term on the right side is the force arising from the bending energy. The second term on the right side is a constraint force required to enforce inextensibility, in which $\mathcal{T}(s,t)$ is a fluctuating tension, or Lagrange multiplier, field. The last term on the right side is a random Brownian force with vanishing mean value and a variance $\langle\boldsymbol{\eta}(s,t)\boldsymbol{\eta}(s',t')\rangle = 2k_BT\boldsymbol{\zeta}(s,t)\delta(s-s')\delta(t-t')$. Solutions of Eq. (2) must satisfy boundary conditions requiring that $\partial^2\mathbf{r}/\partial s^2 = \partial^3\mathbf{r}/\partial s^3 = \mathcal{T} = 0$ at both chain ends.

This free-draining model ignores the effects of long range hydrodynamic interactions. The theory of slender body hydrodynamics [e.g., Batchelor (1970)] shows that, in the limit of a rodlike object of length L much greater than its hydrodynamic diameter d, the effects of hydrodynamic drag can be mimicked, to within logarithmic corrections, by the use of an anisotropic local friction, with coefficients $\zeta_\perp = 2\zeta_\parallel \simeq 4\pi\eta_s$, where η_s is the solvent viscosity. In addition, the theory predicts a weak logarithmic dependence of the effective friction coefficient on the characteristic distance for variation of the drag forces along the chain. For example, the effective friction coefficient for rigid transverse motion of a rod is approximately $4\pi\eta_s/\ln(L/d)$, while that for a bending mode of wavelength $\lambda \gg d$ is approximately $4\pi\eta_s/\ln(\lambda/d)$ [Granek (1997), Kroy and Frey (1997)]. The free-draining model of Eq. (2) ignores this logarithmic scale dependence, but does allow us to retain the factor of 2 difference between $\zeta_\parallel$ and $\zeta_\perp$ when comparing to experiment.

B. Time and length scales

We briefly review the characteristic time and length scales relevant to stress relaxation in a solution of semiflexible rods, with $L \ll L_p$ [Morse (1998b)].

The slowest relaxation process in a solution of rods is rotational diffusion. The free draining model described earlier yields a rotational diffusivity $D_{\text{rot}} = 12k_BT/(\zeta_\perp L^3)$, and a corresponding terminal relaxation time

$$\tau_{\text{rod}} = \frac{\zeta_\perp L^3}{72k_BT} \tag{3}$$

for the relaxation of flow-induced anisotropies in the distribution of rod orientations.

The longest wavelength bending mode of a semiflexible rod of length L has a decay time proportional to

$$\tau_\perp \equiv \frac{\zeta_\perp L^4}{\kappa}. \tag{4}$$

This time scale can be estimated by dimensional analysis of Eq. (2), by balancing the frictional force with the bending force. We also define a corresponding time-dependent length scale

$$\xi_\perp(t) \equiv \left(\frac{\kappa t}{\zeta_\perp}\right)^{1/4} \tag{5}$$

which, for $t < \tau_\perp$, is approximately the wavelength of a bending mode with a relaxation time equal to t. Hereafter, the notation $\xi_\perp(\omega) \equiv (\omega\zeta_\perp/\kappa)^{-1/4}$ refers to the same length scale expressed as a function of a frequency $\omega = 1/t$.

Understanding the longitudinal response of a semiflexible rod is the key to understanding the high-frequency viscoelasticity of a solution of rods. At nonzero temperature, a semiflexible rod undergoes thermally excited transverse undulations. As a result, its average end-to-end length is thus always less than its full contour length L, and can be changed slightly by longitudinal forces applied to the chain, without changing the actual contour length, by suppressing (for $\mathcal{T} > 0$) or enhancing (for $\mathcal{T} < 0$) the magnitude of the thermally excited "wrinkles." The resulting effective extensibility can be quantified by an effective longitudinal extension modulus $B \equiv \mathcal{T}/\langle \mathcal{E} \rangle$ measured in a hypothetical experiment in which a uniform infinitesimal tension $\mathcal{T}$ is applied to the chain, and results in an average strain (i.e., fractional change in end-to-end length) $\langle \mathcal{E} \rangle \equiv \langle \delta L \rangle / L$, where $\langle \delta L \rangle$ is the change in the average end-to-end length.

MacKintosh *et al.* (1995) calculated an effective static modulus by using equilibrium statistical mechanics to calculate the longitudinal response to a spatially uniform, static tension. They obtained

$$B \propto \frac{\kappa^2}{k_B T L^3} \tag{6}$$

with a prefactor that depends upon the boundary conditions imposed on the ends of the chain. The effective extensibility of the chain arises from the existence of thermal transverse fluctuations; thus, the modulus increases with decreasing temperature T or increasing rigidity κ. B depends strongly on the chain length, because the calculated compliance $1/B$ is dominated by the contributions of the longest wavelength bending modes.

Subsequently, both Gittes and MacKintosh (1998) and Morse (1998b) calculated a frequency-dependent dynamic longitudinal modulus $B(\omega) = \mathcal{T}(\omega)/\langle \mathcal{E}(\omega) \rangle$, by considering the longitudinal response of a semiflexible rod to a spatially uniform but temporally oscillating tension of complex amplitude $\mathcal{T}(\omega)$ at a frequency ω, and calculating the amplitude $\langle \delta L(\omega) \rangle = L \langle \mathcal{E}(\omega) \rangle$ of the resulting change in the average end-to-end length. Both authors found a modulus

$$\lim_{\omega \gg \tau_\perp^{-1}} B(\omega) = \frac{\kappa^2}{k_B T} \left(\frac{2i\omega\zeta_\perp}{\kappa} \right)^{3/4} \tag{7}$$

at high frequencies, $\omega \gg \tau_\perp^{-1}$, and confirmed that they recovered the static modulus of Eq. (6) at low frequencies, $\omega \ll \tau_\perp^{-1}$. The $\omega^{3/4}$ dependence of $B(\omega)$ at high frequencies can be qualitatively understood as follows: When a chain is subjected to an oscillatory tension with $\omega \gg \tau_\perp^{-1}$, only bending modes with wavelengths shorter $\xi_\perp(\omega)$, which have relaxation rates greater than ω, can respond to the oscillatory tension. Only these short wavelength modes contribute significantly to the extensibility of the chain. To estimate $B(\omega)$, we can thus assume that, for $\omega \gg \tau_\perp^{-1}$, the length $\xi_\perp(\omega)$ replaces the chain length L as the long-wavelength cutoff in Eq. (6). This scaling argument gives

$$B(\omega) \sim \frac{\kappa^2}{k_B T \xi_\perp^3(\omega)} \tag{8}$$

in agreement with Eq. (7).

The slight longitudinal extensibility of a semiflexible rod gives rise to a nontrivial longitudinal dynamics [Morse (1998b), Everaers *et al.* (1999)]. We have noted previously [Morse (1998b), Pasquali *et al.* (2001)] that the average longitudinal force balance for a semiflexible rod with a frequency-dependent longitudinal modulus $B(\omega)$ can be recast in the form of a modified diffusion equation for the average tension $\langle \mathcal{T}(s,\omega) \rangle$, with a frequency-dependent diffusivity $D(\omega) = B(\omega)/\zeta$. This yields a kind of anomolous diffusion in which tension and longitudinal strain propagate a distance

$$\xi_\parallel(t) \equiv \sqrt{\frac{|B(1/t)|t}{\zeta_\parallel}} = \left[\left(\frac{2\zeta_\perp}{\zeta_\parallel} \right)^3 \frac{k_B T L_p^5}{\zeta_\parallel} t \right]^{1/8} \tag{9}$$

in a time t, giving $\xi_\parallel(t) \propto t^{1/8}$. The notation $\xi_\parallel(\omega) \equiv \sqrt{|B(\omega)|/(\omega\zeta_\parallel)}$ denotes the same length as a function of $\omega = 1/t$. Setting $\xi_\parallel(t) = L$ yields a characteristic time scale

$$\tau_\parallel \equiv \left(\frac{\zeta_\parallel}{2\zeta_\perp} \right)^3 \frac{\zeta_\parallel L^8}{k_B T L_p^5} \tag{10}$$

required for strain and tension to diffuse the entire length of the chain, which is also the time required for the chain length to relax significantly after a sudden deformation.

Equations (3), (4), and (10) yield ratios of the time scales $\tau_{\rm rod}, \tau_\perp$, and $\tau_\parallel$:

$$\frac{\tau_\parallel}{\tau_\perp} \propto \left(\frac{L}{L_p} \right)^4, \quad \frac{\tau_\perp}{\tau_{\rm rod}} \propto \frac{L}{L_p}. \tag{11}$$

These three time scales thus become well separated in the rodlike limit $L \ll L_p$, and form a hierarchy $\tau_\parallel \ll \tau_\perp \ll \tau_{\rm rod}$. The dynamical response of a solution of such rods is therefore expected to exhibit three time regimes in an experiment, such as a step strain, that subjects the system to a sudden perturbation: At early times, $t \ll \tau_\parallel$, the end-to-end length has insufficient time to relax significantly and so will retain the value imposed on it by the initial perturbation. At intermediate times, $\tau_\parallel \ll t \ll \tau_\perp$, the longitudinal deformation of the chains has had time to undergo significant (but not necessarily complete) relaxation, but the longest wavelength bending modes have not yet relaxed. At late times, $t > \tau_\perp$, both longitudinal and transverse degrees of freedom are fully relaxed, and the polymer behaves like a rigid rod. Note that the width of the intermediate regime grows rapidly with decreasing L/L_p, but that the gaps between $\tau_\parallel, \tau_\perp$, and $\tau_{\rm rod}$ disappear as L approaches L_p from below, causing the intermediate regime to vanish.

C. Stress relaxation

Here we discuss some qualitative features of the relaxation of stress $\boldsymbol{\sigma}(t) = G(t)[\boldsymbol{\gamma}_0 + \boldsymbol{\gamma}_0^T]$ after a step strain of infinitesimal magnitude γ_0 at $t = 0$. In what follows, the polymer contribution to $G(t)$ in a dilute solution of c chains per unit volume will be characterized by an intrinsic relaxation modulus, defined by

$$[G(t)] = \lim_{c \to 0} \frac{G(t) - \delta(t)\eta_s}{c}, \tag{12}$$

which gives the contribution to $G(t)$ per chain and by a corresponding intrinsic dynamic modulus, $[G^*(\omega)] = (G^*(\omega) - i\omega\eta_s)/c$, where $[G^*(\omega)] = i\omega\int_0^\infty dt[G(t)]e^{-i\omega t}$.

We first review the behavior of solutions of true rigid rods [Kirkwood and Auer (1951), Doi and Edwards (1986), Bird *et al.* (1987)]. The stress in a dilute solution of thin rigid rods is given by

$$\boldsymbol{\sigma} = c \int_0^L ds \langle \mathcal{T}(s)\mathbf{uu}\rangle + 3ck_BT\langle \mathbf{uu} - \mathbf{I}/3\rangle, \tag{13}$$

where $\mathcal{T}(s)$ is the tension at point s along a rod, and $\mathbf{u}$ is the unit vector parallel to a rod. The first term on the right-hand-side (rhs) is a viscous stress arising from the tension $\mathcal{T}(s,t)$ that is required to maintain the constraint of inextensibility, which depends linearly on the instantaneous rate of strain $\dot{\boldsymbol{\gamma}}(t)$. The second term is the entropic orientational stress arising from anisotropies in the distribution of rod orientations. For a step strain of magnitude γ_0 at $t = 0$, the rate-of-deformation tensor $\dot{\boldsymbol{\gamma}}(t)$ is a delta-function $\dot{\boldsymbol{\gamma}}(t) = \gamma_0 \delta(t)$. This induces a tension

$$\mathcal{T}(s,t) = \tfrac{1}{2}\zeta_\parallel \delta(t)s(L-s)\boldsymbol{\gamma}_0 : \mathbf{uu}, \tag{14}$$

in a rod with orientation $\mathbf{u}$, with a δ-function time dependence, a parabolic dependence on s, and a magnitude that depends on $\mathbf{u}$. Using this tension to evaluate the viscous tension stress in Eq. (13), averaging the result over chains of different orientations, and calculating the effect of a step strain upon the distribution of rod orientations to obtain the entropic orientational stress, yields an intrinsic modulus

$$[G(t)] = \frac{\zeta_\parallel L^3}{180}\delta(t) + \frac{3}{5}k_BTe^{-t/\tau_\mathrm{rod}}, \tag{15}$$

with a delta-function viscous contribution, and an exponentially decaying orientational contribution that decays by rotational diffusion, with the decay time τ_rod given in Eq. (3). The behavior of $G(t)$ in a solution of semiflexible rods is expected to be similar to that predicted for true rigid rods at late times $t > \tau_\perp$, when all internal deformations have had time to relax. This paper thus focuses on predicting linear viscoelastic behavior at times $t \ll \tau_\perp$, or corresponding frequencies.

Both Gittes and MacKintosh (1998) and Morse (1998b) have predicted that $G^*(\omega)$ in solutions of wormlike chains should vary asymptotically as $G^*(\omega) \propto (i\omega)^{3/4}$ at very high frequencies, or (equivalently) that $G(t) \propto t^{-3/4}$ at very early times. This prediction is based on the assumption that, at sufficiently high frequency in an oscillatory flow, or at sufficiently short times after a step deformation, the frictional coupling between the chain and the solvent will be strong enough to enforce a nearly affine deformation of the end-to-end vector of a chain, i.e., the same longitudinal extension or compression as that experienced by a straight line of ink drawn in the solvent with the orientation of a particular rod. In an oscillatory flow, this affine strain yields a corresponding oscillatory tension with a $\omega^{3/4}$ frequency dependence that directly reflects the frequency dependence of $B(\omega)$. The underlying assumption of an affine longitudinal deformation must break down, however, at frequencies $\omega < \tau_\parallel$, or times $t > \tau_\parallel$, for which the end-to-end length has sufficient time to significantly relax. This earlier prediction is thus expected to be valid only in the high frequency or early time regime.

The behavior of $G(t)$ in the intermediate time regime $\tau_\parallel \ll t \ll \tau_\perp$ is more subtle. We showed in an earlier report on this subject [Pasquali *et al.* (2001)] that the stress is dominated at these intermediate times (as at early times) by a "tension" contribution that arises from the constraint forces, and that both $G(t)$ and the tensions in individual rods decay as $t^{-5/4}$ in this regime. This algebraic decay of the tension at intermediate times is shown here to be an indirect result of the free relaxation of transverse bending modes throughout this time regime: The sequential relaxation of bending modes of increasing wavelength throughout this regime leads to an accordion-like motion, which, as a result of the inextensibility of the chain contour, is found to yield an average longitudinal

strain that relaxes as $t^{-1/4}$. The residual tension induced by frictional forces that oppose the longitudinal component of this motion is proportional to the the time derivative of the strain, and so decays as $t^{-5/4}$.

At late times, $t > \tau_\perp$, the coupled relaxation of the transverse undulations and longitudinal strain is complete, and the macroscopic stress is dominated by a remaining entropic orientational component analogous to that found for rigid rods. This component decays exponential with a decay time τ_{rod} identical (for $L \ll L_p$) to that found for rigid rods.

The above description applies rigorously only to very stiff chains, with $L \ll L_p$. As L approaches L_p from below, the intermediate time regime disappears, leaving an essentially featureless crossover from a $t^{-3/4}$ decay of $G(t)$ at early times to an exponential termain decay. For much longer coil-like chains, with $L \gg L_p$ we expect $G(t)$ to crossover as a function of time from a $t^{-3/4}$ decay at early times to a Rouse-like $t^{-1/2}$ decay at later times. This crossover should occur at a time proportional to $\zeta_\perp L_p^3/(k_B T L_p)$, which is roughly the relaxation time for a bending mode of wavelength L_p, after which the stress relaxation will be controlled by the relaxation of Rouse-like modes with wavelengths greater than L_p.

D. Outline

The rest of this paper is organized as follows. In Sec. II, we expand the equation of motion and related quantities about a rigid rod reference state. In Sec. III we derive an integrodifferential equation relating the average longitudinal tension and strain fields in a semiflexible rod of known orientation, and obtain a formal solution of this relation in terms of a spatially nonlocal longitudinal compliance, or a corresponding nonlocal modulus, which is a generalization of the frequency dependent modulus $B(\omega)$ discussed earlier. In this section, we also introduce an analytically tractable ''local compliance approximation'' that ignores the spatial nonlocality of the relationship between tension and strain, which yields the simple modified diffusion equation for strain that was used in our previous work [Pasquali *et al.* (2001)]. In Sec. IV, we calculate the nonlocal compliance in an approximation that is valid at intermediate- and high-frequencies, $\omega \gg \tau_\perp^{-1}$, the results of which show that the local compliance approximation is also valid throughout the same frequency range. In Sec. V, we use the local compliance approximation to calculate the stress and strain field along a rod in weak flow field. In Sec. VI, we review the formal expression of Morse (1998a) for the stress in a solution of wormlike polymers, and cast this in a form appropriate to a nearly straight rod. In Sec. VII, we use the local compliance approximation to obtain analytic results for the linear viscoelastic moduli for $\omega \gg \tau_\perp^{-1}$. In Sec. VIII, we formulate a more complete theory that is valid in the limit $L \ll L_p$ at arbitrary ω, but that must be evaluated numerically. In Sec. IX, we present Brownian dynamics simulations of semiflexible rods, and compare simulation results for $G(t)$ to the predictions of the full theory. In Sec. X, we compare predictions for $G^*(\omega)$ to experimental data for dilute solutions of poly(benzyl-glutamate). In Sec. XI, we present an accurate analytic approximation to the full theory. In Sec. XII, we compare our theory to that of Harris and Hearst (1966). Conclusions are summarized in Sec. XIII.

The simulations results presented here, and a brief presentation of the local compliance approximation for the tension stress contribution to $G(t)$, have appeared previously in Pasquali *et al.* (2001). Similar simulations of $G(t)$ have also been conducted by Dimitrakopoulos *et al.* (2001). The theoretical treatment of the inextensibility constraint used

here is similar to that used by Liverpool and Maggs (2001) in a recent theoretical study of dynamical light scattering from long semiflexible filaments.

II. EXPANSION ABOUT A ROD

We expand the dynamical equations about a rotating rodlike reference state. Our reference state is a straight rod parallel to a unit vector $\mathbf{n}(t)$ that rotates like a thin non-Brownian rod in a homogeneous velocity gradient

$$\frac{d\mathbf{n}}{dt} = (\mathbf{I} - \mathbf{nn}) \cdot \dot{\boldsymbol{\gamma}} \cdot \mathbf{n}. \tag{16}$$

We expand the polymer contour $\mathbf{r}(s)$ about this line as

$$\mathbf{r}(s,t) = [s + f(s,t)]\mathbf{n}(t) + \mathbf{h}(s,t), \tag{17}$$

where $f(s,t)$ and $\mathbf{h}(s,t)$ are the longitudinal and transverse displacements, respectively. The transverse displacement $\mathbf{h}(s,t)$ always remains orthogonal to $\mathbf{n}(t)$, and can be expanded as

$$\mathbf{h}(s,t) = \sum_{\alpha = 1,2} h_\alpha(s,t)\mathbf{e}_\alpha(t), \tag{18}$$

where $\mathbf{e}_1(t)$ and $\mathbf{e}_2(t)$ are two unit vectors that are always orthogonal to $\mathbf{n}(t)$ and to each other. Greek subscripts are used hereafter to represent transverse directions, and can take values 1 and 2. We choose [following Hinch (1976)] the time evolution of $\mathbf{e}_1(t)$ and $\mathbf{e}_2(t)$ as

$$\frac{d\mathbf{e}_1}{dt} = -\mathbf{n}(\mathbf{e}_1 \cdot \dot{\boldsymbol{\gamma}} \cdot \mathbf{n}), \quad \frac{d\mathbf{e}_2}{dt} = -\mathbf{n}(\mathbf{e}_2 \cdot \dot{\boldsymbol{\gamma}} \cdot \mathbf{n}), \tag{19}$$

so that each transverse basis vector rotates in a plane spanned by itself and $\mathbf{n}(t)$ so as to remain always orthogonal to $\mathbf{n}(t)$.

The constraint of inextensibility, which requires that $|\partial\mathbf{r}(s)/\partial s|^2 = 1$, can be expanded as

$$\left(\frac{\partial f}{\partial s}\right)^2 + 2\frac{\partial f}{\partial s} + \left(\frac{\partial \mathbf{h}}{\partial s}\right)^2 = 0. \tag{20}$$

In the limit $L/L_p \ll 1$, where $|\partial f/\partial s| \ll 1$, this can be expanded, to leading approximation, as

$$\frac{\partial f}{\partial s} \simeq -\frac{1}{2}\left(\frac{\partial \mathbf{h}}{\partial s}\right)^2. \tag{21}$$

It is useful to describe longitudinal displacements in terms of a longitudinal strain field

$$\mathcal{E}(s) \equiv \frac{\partial f}{\partial s} - \left\langle \frac{\partial f}{\partial s} \right\rangle_{\text{eq}}, \tag{22}$$

where $\langle \cdots \rangle_{\text{eq}}$ denotes an average value evaluated in the thermal equilibrium state, i.e., with $\dot{\boldsymbol{\gamma}} = 0$. Using approximation (21), $\mathcal{E}(s)$ can be expressed in terms of transverse displacements as

$$\mathcal{E}(s) \simeq -\frac{1}{2}\left[\left|\frac{\partial \mathbf{h}}{\partial s}\right|^2 - \left\langle\left|\frac{\partial \mathbf{h}}{\partial s}\right|^2\right\rangle_{\text{eq}}\right], \tag{23}$$

to leading order in derivatives of $\mathbf{h}(s)$.

To expand the equation of motion, we substitute expansion (17) for $\mathbf{r}(s,t)$ into Langevin equation (2), while using Eqs. (16) and (19) for the rates of change of $\mathbf{n}(t)$, $\mathbf{e}_1(t)$, and $\mathbf{e}_2(t)$. By projecting the result onto $\mathbf{n}(t)$, $\mathbf{e}_1(t)$, and $\mathbf{e}_2(t)$, we obtain longitudinal and transverse components. The transverse component in direction $\mathbf{e}_\alpha$ is

$$\zeta_\perp\left[\frac{\partial h_\alpha}{\partial t} - \sum_\beta \dot{\gamma}_{\alpha\beta} h_\beta\right] = -\kappa\frac{\partial^4 h_\alpha}{\partial s^4} + \frac{\partial}{\partial s}\left(\mathcal{T}\frac{\partial h_\alpha}{\partial s}\right) + \eta_\alpha, \tag{24}$$

where $\dot{\gamma}_{\alpha\beta} \equiv \mathbf{e}_\alpha \cdot \dot{\boldsymbol{\gamma}} \cdot \mathbf{e}_\beta$, and $\eta_\alpha(s,t) \equiv \mathbf{e}_\alpha(t) \cdot \boldsymbol{\eta}(s,t)$. The longitudinal component is

$$\zeta_\parallel\left[\frac{\partial r_\parallel}{\partial t} - r_\parallel \dot{\boldsymbol{\gamma}} : \mathbf{nn} - \sum_\alpha \dot{\boldsymbol{\gamma}} : (\mathbf{ne}_\alpha + \mathbf{e}_\alpha \mathbf{n}) h_\alpha\right] = -\kappa\frac{\partial^4 r_\parallel}{\partial s^4} + \frac{\partial}{\partial s}\left(\mathcal{T}\frac{\partial r_\parallel}{\partial s}\right) + \eta_\parallel, \tag{25}$$

where $r_\parallel(s,t) \equiv s + f(s,t)$, and $\eta_\parallel(s,t) = \mathbf{n}(t) \cdot \boldsymbol{\eta}(s,t)$. Equations (24) and (25), together with constraint (21), form the equations of motion in the rodlike limit.

III. LONGITUDINAL DYNAMICS

In this section, we derive a formal equation relating the average of the strain and tension fields along a rod of known orientation. We consider the average of longitudinal force balance (25) with respect to rapid fluctuations of f, $\mathbf{h}$, and $\mathcal{T}$ on a semiflexible rod of much more slowly varying orientation $\mathbf{n}$, which is regarded as constant for this purpose. This averaging procedure, which will be denoted by the symbol $\langle\cdots\rangle$ throughout this section, yields

$$\zeta_\parallel\left[\frac{\partial\langle f\rangle}{\partial t} - s\dot{\boldsymbol{\gamma}} : \mathbf{nn}\right] = -\kappa\frac{\partial^4\langle f\rangle}{\partial s^4} + \frac{\partial\langle\mathcal{T}\rangle}{\partial s}. \tag{26}$$

To derive Eq. (26), we have used the fact that the $\langle h_\alpha\rangle = 0$ in Eq. (25) as a result of the invariance of Eq. (24) under the symmetry $\mathbf{h} \to -\mathbf{h}$. Differentiating Eq. (26) with respect to s yields an equivalent relationship

$$\zeta_\parallel\left[\frac{\partial\langle\mathcal{E}\rangle}{\partial t} - \dot{\boldsymbol{\gamma}} : \mathbf{nn}\right] = -\kappa\frac{\partial^4\langle\mathcal{E}\rangle}{\partial s^4} + \frac{\partial^2\langle\mathcal{T}\rangle}{\partial s^2} \tag{27}$$

in terms of the average strain $\langle\mathcal{E}(s,t)\rangle$.

To solve Eq. (27), which relates derivatives of the average strain $\langle\mathcal{E}(s,t)\rangle$ and the average tension $\langle\mathcal{T}(s,t)\rangle$, we need a second relationship between these two fields. This is obtained by combining transverse equation of motion (24) with Eq. (23) for the constraint, which relates the longitudinal strain to the derivatives of $h_\alpha(s)$, by using the transverse equation of motion to calculate the linear response of the average $\langle|\partial\mathbf{h}/\partial s|^2\rangle$ of the quantity that appears on the rhs of Eq. (23) for $\mathcal{E}(s,t)$. We thus consider the solution of transverse Eq. (24) driven by small perturbations arising from the tension field $\mathcal{T}(s,t)$ in the second term on the rhs and also from the velocity gradient tensor $\gamma_{\alpha\beta}$, in the second term on the left-hand-side (lhs). To describe the dynamical linear response of the $\langle\mathcal{E}(s,t)\rangle$ to these perturbations, we must calculate the response of $\langle|\partial\mathbf{h}/\partial s|^2\rangle$ to a temporally oscillating velocity gradient and tension field at arbitrary frequency ω. We hereafter adopt a convention in which Fourier transforms of all time dependent functions

are indicated by replacing the time argument t by a frequency ω, so that, e.g., $\mathcal{E}(s,\omega)$ $\equiv \int dt e^{-i\omega t} \mathcal{E}(s,t)$. In the limit of small perturbations, we expect the responses of $\langle \mathcal{E}(s,\omega) \rangle$ to the velocity gradient and to the tension to be additive, and so expect to be able to write the average strain as a sum

$$\langle \mathcal{E}(s,\omega) \rangle = \Theta(s,\omega)\boldsymbol{\gamma}(\omega){:}\mathbf{nn} + \int_0^L ds' \chi(s,s';\omega)\mathcal{T}(s',\omega) \tag{28}$$

of contributions linear in $\boldsymbol{\gamma}(\omega)$ and $\mathcal{T}(s',\omega)$, with response functions $\Theta(s,\omega)$ and $\chi(s,s';\omega)$ that will be calculated in subsequent sections. The function $\chi(s,s';\omega)$ is a nonlocal longitudinal compliance that gives the average strain induced at point s by a tension applied at s' with frequency ω. The tensor form of the term linear in $\boldsymbol{\gamma}(\omega)$ is dictated by the fact that this contribution to the strain must be a scalar function of $\boldsymbol{\gamma}$ and $\mathbf{n}$ and linear in $\boldsymbol{\gamma}$, and that $\boldsymbol{\gamma}(\omega)$ must be traceless for an incompressible fluid.

A. Full theory

A closed integrodifferential equation for $\langle \mathcal{T}(s,\omega) \rangle$ can be obtained by Fourier transforming Eq. (27) with respect to time and substituting Eq. (28) for $\langle \mathcal{E}(s,\omega) \rangle$, while equating the unspecified tension $\mathcal{T}(s,t)$ in linear response relationship (28) with the average value $\langle \mathcal{T}(s,t) \rangle$ that appears in Eq. (27). This yields

$$\left[i\omega\zeta_\parallel + \kappa \frac{\partial^4}{\partial s^4} \right] \int_0^L ds' \chi(s,s';\omega)\langle \mathcal{T}(s',\omega) \rangle - \frac{\partial^2 \langle \mathcal{T}(s,\omega) \rangle}{\partial s^2} = i\omega\zeta_\parallel \boldsymbol{\gamma}(\omega){:}\mathbf{nn}[1 - \Theta(s,\omega)]. \tag{29}$$

Here and hereafter, $\mathbf{n}(t)$ is approximated by its time average over one period of oscillation. The dimensionless response function $\Theta(s,\omega)$ is calculated in the Appendix, and is found to approach a maximum value proportional to L/L_p in the limit $\omega \gg \tau_\perp^1$. The term involving $\Theta(s,\omega)$ on the rhs of Eq. (29) is thus uniformly smaller than the leading term on the rhs in the limit $L \ll L_p$ of interest, and so can be neglected. Making the derivatives dimensionless by defining $\hat{s} \equiv s/L$ and dividing by $i\omega\zeta_\parallel$ then yields

$$\left(1 + \frac{1}{i\omega\tau_\perp} \frac{\zeta_\perp}{\zeta_\parallel} \frac{\partial^4}{\partial\hat{s}^4} \right) \int_0^L ds' \chi(s,s';\omega)\langle \mathcal{T}(s',\omega) \rangle - \frac{1}{i\omega\zeta_\parallel L^2} \frac{\partial^2 \langle \mathcal{T}(\hat{s},\omega) \rangle}{\partial\hat{s}^2} = \boldsymbol{\gamma}(\omega){:}\mathbf{nn}. \tag{30}$$

An equivalent expression involving the strain, rather than the tension, can be obtained by introducing a nonlocal modulus $B(s,s';\omega)$, defined such that

$$\int_0^L ds' B(s,s';\omega)\chi(s',s'';\omega) = \delta(s-s''), \tag{31}$$

i.e., such that B is the functional inverse of χ. If we consistently neglect the term involving $\Theta(s,\omega)$ in Eq. (28), as done to obtain Eq. (30), we can write $\langle \mathcal{T}(s,\omega) \rangle = \int ds' B(s,s';\omega)\langle \mathcal{E}(s',\omega) \rangle$, to obtain the equivalent expression

$$\left(1 + \frac{1}{i\omega\tau_\perp} \frac{\zeta_\perp}{\zeta_\parallel} \frac{\partial^4}{\partial\hat{s}^4} \right) \langle \mathcal{E}(\hat{s},\psi) \rangle - \frac{1}{i\omega_\parallel L^2} \frac{\partial^2}{\partial\hat{s}^2} \int_0^L ds' B(s,s',\omega)\langle \mathcal{E}(s',\omega) \rangle = \boldsymbol{\gamma}(\omega){:}\mathbf{nn}. \tag{32}$$

Equations (30) and (32) are the starting points for the full theory developed in Sec. VIII.

B. Local compliance approximation

We find in what follows that Eqs. (30) and (32) can be further simplified in the limit of intermediate and high frequencies, $\omega \gg \tau_\perp^1$. First, we note that the coefficient multiplying the fourth derivative term in Eq. (32) is proportional to $(i\omega\tau_\perp)^{-1}$, and that, as result of this small prefactor, is negligible compared to the first term on the left side at all $\omega \gg \tau_\perp^{-1}$. Moreover, we find that the nonlocality of the compliance becomes unimportant at frequencies $\omega \gg \tau_\perp^{-1}$; thus $\chi(s,s';\omega)$ can be approximated at these frequencies by a frequency dependent but spatially local compliance, of the form

$$\chi(s,s';\omega) \simeq \chi(\omega)\delta(s-s'). \tag{33}$$

Here $\chi(\omega) = 1/B(\omega)$, where $B(\omega)$ is the frequency-dependent modulus given in Eq. (7), which was obtained by calculating the spatial average strain induced by a spatially uniform tension at frequencies $\omega \gg \tau_\perp^{-1}$. The resulting local compliance approximation (LCA) assumes that the average strain and tension are locally proportional, so that

$$\langle \mathcal{E}(s,\omega)\rangle = \chi(\omega)\langle \mathcal{T}(s,\omega)\rangle. \tag{34}$$

Substituting this approximation in Eq. (27), and neglecting the fourth derivative term, yields the LCA longitudinal balance equation

$$\left[i\omega - \frac{B(\omega)}{\zeta_\parallel}\frac{\partial^2}{\partial s^2}\right]\langle \mathcal{E}(s,\omega)\rangle = \dot{\gamma}(\omega)\!:\!\mathbf{nn}, \tag{35}$$

where $\dot{\gamma}(\omega) \equiv i\omega\gamma(\omega)$.

Equation (35) has the form of a diffusion equation, with a frequency-dependent diffusivity $D(\omega) \equiv B(\omega)/\zeta_\parallel$, and a spatially uniform source term arising from the rate of straining along direction $\mathbf{n}$. An analytic solution to this diffusion equation, which satisfies the boundary condition $\langle \mathcal{T}(s,\omega)\rangle = 0$ at the chain ends, is presented in Sec. V. At high frequencies, $\omega \gg \tau_\parallel^{-1}$, for which $\xi_\parallel(\omega) \ll L$, the solution of Eq. (35) is found to yield tension and strain fields that vary over lengths of order the longitudinal diffusion length $\xi_\parallel(\omega)$, as suggested by dimensional analysis. At intermediate frequencies, $\tau_\perp^{-1} \ll \omega \ll \tau_\parallel^{-1}$, for which $L \ll \xi_\parallel(\omega)$, the tension and strain are found to vary smoothly over the entire chain length L.

To justify the LCA, the predicted characteristic distances for spatial variations of $\langle \mathcal{T}(s,\omega)\rangle$ at each frequency must be compared to the calculated range of the nonlocality of $\chi(s,s';\omega)$: The approximation of $\chi(s,s';\omega)$ by a δ function is justified only if the predicted $\langle \mathcal{T}(s,\omega)\rangle$ varies slowly over distances comparable to the range of values of $|s-s'|$ for which $\chi(s,s';\omega)$ remains significant. In Sec. IV, $\chi(s,s';\omega)$ is calculated in an approximation valid at $\omega \gg \tau_\perp^{-1}$, and it is shown that $\chi(s,s';\omega)$ has a range of nonlocality proportional to the transverse length $\xi_\perp(\omega)$. Using this result, the validity of the LCA can be justified at all $\omega \gg \tau_\perp^{-1}$ by using Eqs. (4) and (10) to confirm that $\xi_\perp(\omega) \ll \xi_\parallel(\omega)$ throughout the high-frequency $\omega \gg \tau_\parallel^{-1}$ regime in which the tension varies over distances of order $\xi_\parallel(\omega)$, and that $\xi_\perp(\omega) \ll L$ throughout the intermediate regime $\tau_\parallel^{-1} \gg \omega \gg \tau_\perp^{-1}$ in which the tension varies smoothly over the entire chain length. The LCA fails at frequencies comparable to and less than $\tau_\perp^{-1}$, however, for which the nonlocality of $\chi(s,s';\omega)$ extends over the full chain length.

IV. NONLOCAL COMPLIANCE AT INTERMEDIATE AND HIGH FREQUENCIES

We now calculate $\chi(s,s';\omega)$ in an approximation appropriate to the limit $\xi_\perp(\omega)$ $\ll L$ or, equivalently, $\omega \gg \tau_\perp^{-1}$. In this limit, the calculation of $\chi(s,s';\omega)$ from the transverse equation of motion becomes insensitive to the finite length of the chain, and so the calculation can be performed as if the chain were infinite, by using an expression of $h_\alpha(s)$ in a continuous distribution of Fourier modes

$$h_\alpha(s,t) = \int \frac{dq}{2\pi} h_\alpha(q,t) e^{-iqs}, \tag{36}$$

with amplitudes $h_\alpha(q,t) = \int ds\, h_\alpha(s,t) e^{iqs}$. The bending energy of Eq. (1) can be expanded to quadrative order in Fourier amplitudes as

$$U_{\text{bend}} = \frac{1}{2} \sum_\alpha \int \frac{dq}{2\pi} \kappa q^4 |h_\alpha(q)|^2. \tag{37}$$

Fourier transforming Eq. (24) yields a transformed transverse equation of motion

$$\left(\zeta_\perp \frac{\partial}{\partial t} + \kappa q^4 \right) h_\alpha(q) = \zeta_\perp \sum_\beta \dot{\gamma}_{\alpha\beta} h_\beta(q) - \int \frac{dq_1}{2\pi} q(q-q_1) \mathcal{T}(q_1) h_\alpha(q-q_1) + \eta_\alpha(q), \tag{38}$$

where $\mathcal{T}(q,t)$ and $\eta_\alpha(q,t)$ are the corresponding spatial Fourier transforms of $\mathcal{T}(s,t)$ and $\eta_\alpha(s,t)$, respectively, and the random force satisfies $\langle \eta_\alpha(q,t) \rangle = 0$ and $\langle \eta_\alpha(q,t) \eta_\beta(q',t') \rangle = \delta_{\alpha\beta} 2\pi \delta(q+q') \delta(t-t') 2 k_B T \zeta_\perp$.

To calculate the nonlocal compliance, we calculate the linear response of the average strain $\langle \mathcal{E}(k,t) \rangle$ to a prescribed tension, where $\langle \cdots \rangle$ is used in this section to represent an average over different realizations of the transverse noise. Fourier transforming Eq. (23) for $\mathcal{E}(s,t)$, yields

$$\langle \mathcal{E}(k,t) \rangle = \int \frac{dq}{2\pi} q(k-q) a(q,k;t), \tag{39}$$

where

$$a(q,k;t) \equiv \frac{1}{2} \sum_\alpha \left[\langle h_\alpha(q) h_\alpha(k-q) \rangle - \langle h_\alpha(q) h_\alpha(k-q) \rangle_{\text{eq}} \right]. \tag{40}$$

The time derivative of $a(q,k;t)$ is calculated by using Eq. (38) to evaluate

$$\frac{\partial a(q,k;t)}{\partial t} = \frac{1}{2} \sum_\alpha \left\langle \frac{\partial h_\alpha(q)}{\partial t} h_\alpha(k-q) + h_\alpha(q) \frac{\partial h_\alpha(k-q)}{\partial t} \right\rangle, \tag{41}$$

while setting $\dot{\gamma}_{\alpha\beta} = 0$ on the first term on the rhs of Eq. (38). To evaluate the rhs of Eq. (41), we approximate averages of the form $\langle h_\alpha(q,t) h_\beta(q',t) \rangle$ that appear multiplied by explicit factors of $\mathcal{T}(-q-q')$ by their equilibrium values, for the purpose of calculating the linear response to $\mathcal{T}$, using the equilibrium variance $\langle h_\alpha(q_1) h_\beta(q_2) \rangle_{\text{eq}}$ $= \delta_{\alpha\beta} 2\pi \delta(q_1+q_2) k_B T / \kappa q_1^4$, which is obtained by applying the equipartition theorem to Eq. (37). We also use the identify $\langle \eta_\alpha(q_1) h_\beta(q_2) \rangle = k_B T \delta_{\alpha\beta} 2\pi \delta(q_1+q_2)$ for terms involving the random force [see, for example, Doi and Edwards (1986) p. 112]. This yields the differential equation

$$\left\{\zeta_\perp \frac{\partial}{\partial t} + \kappa[q^4+(k-q)^4]\right\}a(q,k;t) = \mathcal{T}(k,t)\left[\frac{q}{(k-q)^3}+\frac{(k-q)}{q^3}\right]\frac{k_BT}{\kappa}. \tag{42}$$

Fourier transforming Eq. (42) with respect to time yields a corresponding algebraic equation

$$a(q,k;\omega) = \frac{\mathcal{T}(k,\omega)}{i\omega\zeta_\perp + \kappa[q^4+(k-q)^4]}\left[\frac{q}{(k-q)^3}+\frac{(k-q)}{q^3}\right]\frac{k_BT}{\kappa}, \tag{43}$$

for $a(q,k;\omega) \equiv \int dt\, e^{-i\omega t}a(q,k;t)$, where $\mathcal{T}(k,\omega)$ is the corresponding Fourier transform of $\mathcal{T}(k,t)$. Finally, substituting Eq. (43) for $a(q,k;\omega)$ into the temporal Fourier transform of Eq. (39) gives a strain of the form

$$\langle\mathcal{E}(k,\omega)\rangle = \chi(k,\omega)\mathcal{T}(k,\omega), \tag{44}$$

where

$$\chi(k,\omega) = \frac{k_BT}{\kappa}\int\frac{dq}{2\pi}\frac{1}{i\omega\zeta_\perp + \kappa[q^4+(k-q)^4]}\left[\frac{q^2}{(k-q)^2}+\frac{(k-q)^2}{q^2}\right] \tag{45}$$

is a k- and ω-dependent nonlocal compliance.

Prior results for the response to a spatially uniform tension can be recovered by evaluating $\chi(k,\omega)$ at $k = 0$, which we denote by a function $\chi(\omega) \equiv \chi(k = 0,\omega)$. This yields

$$\chi(\omega) = \frac{k_BT}{\kappa}\int_{q \sim 1/L}\frac{dq}{2\pi}\frac{1}{\frac{i}{2}\omega\zeta_\perp + \kappa q^4}. \tag{46}$$

The lower limit of integration is included as a reminder that the existence of a finite chain length L imposes a cutoff on the range of allowable wave numbers. At frequencies $\omega \gg \tau_\perp^{-1}$, where the calculation given in this section is valid, the integral is insensitive to this lower cutoff, and yields

$$\lim_{\omega \gg \tau_\perp^{-1}}\chi(\omega) = \frac{k_BT}{\kappa^2}\left(\frac{2i\omega\zeta_\perp}{\kappa}\right)^{-3/4}, \tag{47}$$

in agreement with results of Gittes and MacKintosh (1998) and Morse (1998b) for $B(\omega) \equiv 1/\chi(\omega)$. For $\omega \ll \tau_\perp^{-1}$, the integral in Eq. (46) instead is controlled by its lower limit, indicating that the calculation is no longer quantitatively valid, as a result of our use of a continuous distribution of Fourier modes rather than discrete bending modes to expand $h_\alpha(s)$. However, a scaling relation can be obtained by using a lower cutoff proportional to $1/L$, which yields $\chi(\omega) \propto k_BTL^3/\kappa^2$, in agreement with the result of MacKintosh et al. (1995) for the static compliance.

The wavenumber dependence of $\chi(k,\omega)$ at frequencies $\omega \gg \tau_\perp^{-1}$ can be made more transparent by rewriting Eq. (45) in the scaling form

$$\chi(k,\omega) = \chi(\omega)F(k\xi_\perp(\omega)), \tag{48}$$

where $\chi(\omega)$ is given by Eq. (46), and

$$F(\hat{k}) \equiv 2^{3/4}\int\frac{d\hat{q}}{2\pi}\frac{1}{i+\hat{q}^4+(\hat{k}-\hat{q})^4}\left[\frac{\hat{q}^2}{(\hat{k}-\hat{q})^2}+\frac{(\hat{k}-\hat{q})^2}{\hat{q}^2}\right], \tag{49}$$

where $\hat{q} \equiv q\xi_\perp(\omega)$ and $\hat{k} \equiv k\xi_\perp(\omega)$, and where $F(0) = 1$. Carrying out an inverse spatial transform of Eq. (48) yields a corresponding nonlocal compliance of the form

$$\chi(s-s',\omega) = \chi(\omega)\tilde{F}\left(\frac{s-s'}{\xi_\perp(\omega)}\right), \tag{50}$$

where $\tilde{F}(x)$ is the inverse Fourier transform of $F(\hat{k})$. The existence of this scaling form shows that, at a given frequency ω, $\chi(s,s';\omega)$ depends only on the ratio $|s-s'|/\xi_\perp(\omega)$, and thus has a range proportional to $\xi_\perp(\omega)$. Using this fact, the LCA can be shown to be a consistent approximation at all $\omega \gg \tau_\perp^{-1}$ because it leads to a tension $\langle\mathcal{T}(s,\omega)\rangle$ that varies slowly over distances of order $\xi_\perp(\omega)$ at these frequencies.

V. TENSION AND STRAIN IN THE LCA

In this section, we use the LCA to calculate the average strain and tension fields along a rod of known orientation **n** in a solvent subjected to a weak oscillatory or step strain. To begin, we rewrite Eq. (35) in dimensionless form as

$$\left\{1 - \frac{1}{\lambda^2(\omega)}\frac{\partial^2}{\partial\hat{s}^2}\right\}\langle\mathcal{E}(s,\omega)\rangle = \boldsymbol{\gamma}(\omega):\mathbf{nn}, \tag{51}$$

where $\hat{s} \equiv s/L$ is dimensionless arc length, and where we have introduced a complex dimensionless parameter

$$\lambda(\omega) \equiv \left[\frac{i\omega\zeta_\parallel L^2}{B(\omega)}\right]^{1/2} = (i\omega\tau_\parallel)^{1/8} = i^{1/8}\frac{L}{\xi_\parallel(\omega)}. \tag{52}$$

The parameter $\lambda(\omega)$ characterizes the relative importance of the first term on the lhs of Eq. (51), which arises from longitudinal drag forces, relative to the second derivative term, which arises from forces produced by gradients in $\langle\mathcal{T}(s,\omega)\rangle$. [This definition of $\lambda(\omega)$ differs by a factor of 2 from that used in Pasquali *et al.* (2001)]. Equation (51) can be solved exactly subject to the boundary condition that the average tension (and hence the average strain) vanishes at the chain ends $\hat{s} = 0$ and $\hat{s} = 1$:

$$\langle\mathcal{E}(s,\omega)\rangle = \left\{1 - \frac{\cosh[\lambda(\omega)(\hat{s}-\frac{1}{2})]}{\cosh[\lambda(\omega)/2]}\right\}\boldsymbol{\gamma}(\omega):\mathbf{nn}. \tag{53}$$

The corresponding tension is given in the LCA by $\mathcal{T}(s,\omega)\rangle = B(\omega)\langle\mathcal{E}(s,\omega)\rangle$.

Hereafter we focus on the response to oscillatory strains of magnitude $\boldsymbol{\gamma}(\omega)$, which can be directly described by Eq. (53), and to step strains $\boldsymbol{\gamma}(t) = \boldsymbol{\gamma}_0\Theta(t)$ of magnitude $\boldsymbol{\gamma}_0$ at $t = 0$, which must be treated by inverse Fourier transformation of Eq. (53). To treat the latter problem, we note that such a step strain yields a rate of strain $\dot{\boldsymbol{\gamma}}(t) = \boldsymbol{\gamma}_0\delta(t)$ whose Fourier transform $\dot{\boldsymbol{\gamma}}(\omega) = i\omega\boldsymbol{\gamma}(\omega) = \boldsymbol{\gamma}_0$ is independent of ω, giving Fourier amplitudes $\boldsymbol{\gamma}(\omega) = \dot{\boldsymbol{\gamma}}(\omega)/(i\omega) = \boldsymbol{\gamma}_0/(i\omega)$. To clarify the physical content of Eq. (53), it is useful to consider separately the high-frequency limit where $\lambda(\omega) \gg 1$, corresponding to $\omega \gg \tau_\parallel^{-1}$, and the intermediate regime where $\lambda(\omega) \ll 1$, corresponding to $\tau_\parallel^{-1} \gg \omega \gg \tau_\perp^{-1}$.

A. High frequencies and short times

We first consider the limiting behavior of the $\langle\mathcal{E}(s,\omega)\rangle$ and $\langle\mathcal{T}(s,\omega)\rangle$ in an oscillatory flow at frequencies $\omega \gg \tau_\parallel^{-1}$, where $\lambda(\omega) \gg 1$. In this limit, the first term on the left side
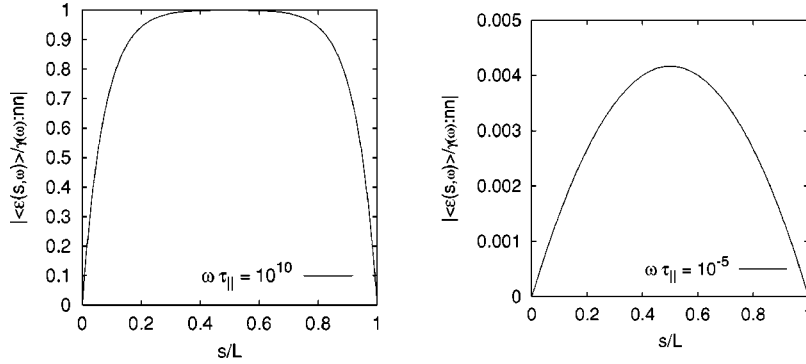
FIG. 1. Magnitude of the average strain $\langle \mathcal{E}(s,\omega) \rangle$, normalized by the affine strain $\gamma(\omega)$:**nn**, as a function of $\hat{s} = s/L$, as calculated from the local compliance approximation [Sec. V, Eq. (53)], for $\omega \tau_\parallel = 10^{10}$ (left panel) and $\omega \tau_\parallel = 10^{-5}$ (right panel).

of Eq. (51), representing the drag force, is much larger than the second derivative term. Balancing this drag force against the extensional strain on the rhs yields a spatially uniform average strain

$$\langle \mathcal{E}(s,\omega) \rangle \simeq \gamma(\omega):\mathbf{nn}. \tag{54}$$

This is simply the affine strain that would be experienced by a line of ink drawn in the fluid. In the LCA, this yields a corresponding spatially uniform tension

$$\langle \mathcal{T}(s,\omega) \rangle \simeq B(\omega)\gamma(\omega):\mathbf{nn} \tag{55}$$

that, for fixed strain amplitude, grows as $\omega^{3/4}$. Because the boundary conditions require that $\mathcal{T}(s,\omega) = 0$ at the chain ends, however, there must be a narrow boundary layer near each chain end where the average strain and tension drop from these uniform values to zero; there the second derivative term in Eq. (51) must remain important. The thickness of the boundary layer is given by the distance $\xi_\parallel(\omega) \propto \omega^{-1/8}$ over which tension can diffuse in a time $1/\omega$. This behavior is shown in the left panel of Fig. 1, where the magnitude of the exact solution (53) is plotted at a reduced frequency of $\omega\tau_\parallel = 10^{10}$. The boundary layers remain rather wide even at this extremely high frequency because $\xi_\parallel(\omega)$ decays only as $\omega^{-1/8}$.

The decay of the tension at correspondingly early times $t \ll \tau_\parallel$ after a small step strain can be obtained by inverse Fourier transformation of Eq. (55), using Fourier amplitudes $\gamma(\omega) = \gamma_0/(i\omega)$. This yields

$$\langle \mathcal{T}(s,t) \rangle = \int \frac{d\omega}{2\pi} \frac{B(\omega)}{i\omega} e^{i\omega t} \gamma_0 :\mathbf{nn} \tag{56}$$

everywhere outside of the boundary layers near the chain ends. Noting that $B(\omega) \propto (i\omega)^{3/4}$, one finds, either by power counting or by evaluating the integral, that $\mathcal{T}(t)$ remains nearly spatially uniform outside the boundary layers near the chain ends, and decays with time as

$$\mathcal{T}(t) \propto t^{-3/4}. \tag{57}$$

The corresponding strain $\langle \mathcal{E}(s,t) \rangle$ is also found to remain nearly uniform outside the boundary layers, and to approximately retain the value $\mathcal{E}(s,t) = \gamma_0 :\mathbf{nn}$ produced by the initial affine deformation.

B. Intermediate frequencies and times

We now consider the behavior in oscillatory flow at intermediate frequencies $\tau_\parallel^{-1}$ $\gg \omega \gg \tau_\perp^{-1}$, for which $\lambda(\omega) \ll 1$, but for which the LCA still remains valid. In this regime the dominant balance in Eq. (51) is between the extensional strain on the rhs and the second derivative term on the lhs. The limit $\lambda(\omega) \to 0$ can be obtained by setting $B(\omega) \to \infty$. To leading order in $\lambda(\omega)$, the behavior found in this regime is thus identical to that found for an inextensible rigid rod. However, we find that the first order correction to this result must be analyzed to understand adequately the qualitative behavior of the stress in this regime. We thus expand the tension as a perturbation series

$$\langle \mathcal{T}(s,\omega) \rangle = \langle \mathcal{T}_0(s,\omega) \rangle + \langle \mathcal{T}_1(s,\omega) \rangle + \cdots \tag{58}$$

where each subsequent term is smaller than the previous by a factor the small parameter $[\lambda(\omega)]^2$, or $(i\omega\tau_\parallel)^{1/4}$, and $\mathcal{T}_0(s,\omega)$ is the asymptotic behavior obtained by setting $\lambda(\omega) \to 0$, or $B(\omega) \to \infty$.

The leading contribution $\langle \mathcal{T}_0 \rangle$ can be obtained by ignoring the first term on the lhs of Eq. (35), while setting $\langle \mathcal{T}_0(s,\omega) \rangle = B(\omega)\langle \mathcal{E}(s,\omega) \rangle$ in the second. This yields a differential equation

$$\frac{\partial^2 \langle \mathcal{T}_0(s,\omega) \rangle}{\partial \hat{s}^2} = -i\omega\zeta_\parallel L^2 \boldsymbol{\gamma}(\omega):\mathbf{nn}, \tag{59}$$

whose solution gives

$$\langle \mathcal{T}_0(s,\omega) \rangle = \tfrac{1}{2} i\omega\zeta_\parallel L^2 \hat{s}(1-\hat{s})\boldsymbol{\gamma}(\omega):\mathbf{nn}. \tag{60}$$

This leading order tension is identical to that obtained for a rigid rod, which varies linearly with the rate of strain $\dot{\boldsymbol{\gamma}}(\omega) = i\omega\boldsymbol{\gamma}(\omega)$. In a semiflexible chain, unlike a rigid rod, this leading order tension induces a nonzero leading order strain $\langle \mathcal{E}_0(s,\omega) \rangle \equiv \langle \mathcal{T}_0(s,\omega) \rangle / B(\omega)$. Equation (8) for $B(\omega) \propto (i\omega)^{3/4}$ yields a strain

$$\langle \mathcal{E}_0(s,\omega) \rangle = \tfrac{1}{2}(i\omega\tau_\parallel)^{1/4}\hat{s}(1-\hat{s})\boldsymbol{\gamma}(\omega):\mathbf{nn} \tag{61}$$

that varies as $\omega^{1/4}$ with frequency, with the same parabolic dependence on $\hat{s}$ as the tension. This strain is small compared to the affine strain $\boldsymbol{\gamma}(\omega):\mathbf{nn}$ when $\omega \ll \tau_\parallel^{-1}$, and become comparable in magnitude to the affine strain when $\omega \sim \tau_\parallel^{-1}$. This small parabolic strain is shown in the right panel of Fig. 13, where the magnitude of the exact solution is plotted for a reduced frequency $\omega\tau_\parallel = 10^{-5}$.

Next, we consider the decay of the leading order tension and strain in the intermediate time regime $\tau_\parallel \ll t \ll \tau_\perp$ after a step deformation. The leading order tension, which can be obtained by inverse Fourier transforming Eq. (60), is identical to that given in Eq. (14) for a rigid rod

$$\langle \mathcal{T}_0(s,t) \rangle = \tfrac{1}{2}\delta(t)\zeta_\parallel L^2 \hat{s}(1-\hat{s})\boldsymbol{\gamma}_0:\mathbf{nn}, \tag{62}$$

and has a delta-function time dependence. The ''leading order'' contribution to $\langle \mathcal{T}(s,t) \rangle$ in the intermediate time regime, if defined as the inverse Fourier transform of the leading order contribution to $\langle \mathcal{T}(s,\omega) \rangle$ in the corresponding frequency regime, thus vanishes in the time domain $\tau_\parallel \ll t \ll \tau_\perp$ of interest. However, the associated leading order longitudinal strain $\langle \mathcal{E}_0(s,t) \rangle$ induced by this tension does not vanish at intermediate times, and can be calculated by Fourier transforming Eq. (61) for $\langle \mathcal{E}_0(s,\omega) \rangle$. Evaluating (or power counting) the resulting Fourier integral, using Fourier components $\boldsymbol{\gamma}(\omega) = \boldsymbol{\gamma}_0/(i\omega)$, yields a strain

$$\langle \mathcal{E}_0(s,t)\rangle \sim (t/\tau_\parallel)^{-1/4}\hat{s}(1-\hat{s})\boldsymbol{\gamma}_0:\mathbf{nn} \tag{63}$$

that decays with time as $t^{-1/4}$. This is the strain induced by the δ-function impulse of tension given by Eq. (62). This impulse creates a nonequilibrium distribution of bending mode amplitudes at the beginning of the intermediate time regime, creating a strain that relaxes via the free relaxation of bending modes of increasing wavelength throughout the intermediate time regime. The rate of decay of the longitudinal strain in the intermediate time regime is thus limited primarily by the rate of free decay of the bending modes, rather than by resistance to longitudinal motion, and is completed only when the slowest bending mode relaxes.

Because the leading order approximation for the tension vanishes at times $\tau_\parallel \ll t \ll \tau_\perp$, the tension in this regime is dominated by the first order correction $\langle \mathcal{T}_1(s,t)\rangle$. To calculate this correction, we again start in the frequency domain, and expand Eq. (51) to first order in $\lambda^2(\omega)$, using the zeroth order solution to cancel all zeroth order terms. By this method, we find that $\langle \mathcal{T}_1(s,\omega)\rangle$ must satisfy

$$\frac{\partial^2\langle \mathcal{T}_1(s,\omega)\rangle}{\partial s^2} = i\omega\zeta_\parallel\langle \mathcal{E}_0(s,\omega)\rangle \tag{64}$$

or, equivalently, that

$$\frac{\partial^2\langle \mathcal{T}_1(s,t)\rangle}{\partial s^2} = \zeta_\parallel\frac{\partial\langle \mathcal{E}_0(s,t)\rangle}{\partial t} \tag{65}$$

in the time domain. Equations (64) and (65) show that $\langle \mathcal{T}_1(s,t)\rangle$ is the tension required to balance the longitudinal frictional force that opposes relaxation of the zeroth order longitudinal strain $\langle \mathcal{E}_0(s,t)\rangle$. This residual tension has a subdominant effect on the relaxation of the strain, but is important because it is found in Sec. VII to yield the dominant contribution to $G(t)$ at intermediate times. Solving Eqs. (64) and (65) yields

$$\langle \mathcal{T}_1(s,\omega)\rangle = \frac{1}{12}\zeta_\parallel L^2(i\omega)^{5/4}\tau_\parallel^{1/4}\left(-\frac{\hat{s}}{2}+\hat{s}^3-\frac{\hat{s}^4}{2}\right)\boldsymbol{\gamma}(\omega):\mathbf{nn} \tag{66}$$

in an oscillatory flow, or

$$\langle \mathcal{T}_1(s,t)\rangle \propto t^{-5/4}\left(-\frac{\hat{s}}{2}+\hat{s}^3-\frac{\hat{s}^4}{2}\right)\boldsymbol{\gamma}_0:\mathbf{nn} \tag{67}$$

following a step deformation. This residual tension decays as $t^{-5/4}$ because, by Eq. (65), the first order tension is proportional to the time derivative of the leading order strain, which decays as $t^{-1/4}$.

VI. STRESS TENSOR

The intramolecular polymer contribution to the stress is given, for any discrete model of beads interacting via an intramolecular potential energy, by the Kramer–Kirkwood expression [Doi and Edwards (1986)]:

$$\boldsymbol{\sigma}_p \equiv \frac{-1}{V}\sum_{i=1}^N \langle \mathbf{R}_i\mathbf{F}_i\rangle, \tag{68}$$

where $\mathbf{R}_i$ is the position of bead i, $\mathbf{F}_i = -\partial[U+k_BT\ln\Psi]/\partial\mathbf{R}_i$ is the effective force on bead i, $U(\{\mathbf{R}\})$ is an intramolecular potential energy, and $\Psi(\{\mathbf{R}\})$ is a single chain prob-

ability distribution function. An expression for the intramolecular stress in a solution of wormlike chains has been obtained by Morse (1998a) by applying the Kramers–Kirkwood formula to a discretized model of a wormlike chain as a chain of N beads connected by very stiff springs with a preferred distance a between neighboring beads, with a three-body bending potential that is a discretized version of bending energy (1). By evaluating the rhs of Eq. (68) for this discrete model, then taking the limit $a \ll L_p$ of continuous, weakly curved chains, and re-expressing the results in terms of a continuous arc length variable $s = ia$, Morse (1998a) obtained a stress

$$\boldsymbol{\sigma}_p = \boldsymbol{\sigma}_{\text{curv}} + \boldsymbol{\sigma}_{\text{tens}} + \boldsymbol{\sigma}_{\text{ornt}} - ck_BT\mathbf{I}, \tag{69}$$

where

$$\boldsymbol{\sigma}_{\text{tens}} = c \int_0^L ds \langle \mathcal{T}\mathbf{uu}\rangle, \tag{70}$$

$$\boldsymbol{\sigma}_{\text{curv}} = c\kappa \int_0^L ds \left\langle \frac{\partial\mathbf{u}}{\partial s}\frac{\partial\mathbf{u}}{\partial s} - \mathbf{uu}\left|\frac{\partial\mathbf{u}}{\partial s}\right|^2 \right\rangle + \frac{ck_BT}{a}\int_0^L ds \langle 3\mathbf{uu} - \mathbf{I}\rangle, \tag{71}$$

$$\boldsymbol{\sigma}_{\text{ornt}} = \tfrac{3}{2}ck_BT\langle \mathbf{u}(0)\mathbf{u}(0) + \mathbf{u}(L)\mathbf{u}(L) - \tfrac{2}{3}\mathbf{I}\rangle, \tag{72}$$

where $\mathbf{u} = \mathbf{u}(s)$ and $\mathcal{T} = \mathcal{T}(s)$ are the unit tangent and tension for a bond at position $s = ia$. The physical meaning of these three stress contributions (briefly) is: The "tension stress" $\boldsymbol{\sigma}_{\text{tens}}$ arises from the constraint forces that enforce inextensibility in the chain. The "curvature stress" $\boldsymbol{\sigma}_{\text{curv}}$ contains both a purely mechanical contribution arising from the bending forces [the first term on the rhs of Eq. (71)] and an entropic contribution arising from the orientational entropy of the links (the second term). The curvature stress was shown, using the underlying discrete model, to vanish in a hypothetical partially equilibrated state in which the variance of the curvature at each point on the chain retains its thermal equilibrium value, or, for a rodlike polymer, in which the distribution of bending mode amplitudes is equilibrated. The curvature stress thus arises from disturbances of this equilibrium distribution of bending mode amplitudes. The "orientational stress" $\boldsymbol{\sigma}_{\text{ornt}}$ is a residual contribution of the orientational entropy arising from the two end links.

These expressions can be further simplified in the rodlike limit. In this limit, to leading order, $\mathbf{u}(s)$ can be approximated by the global rod orientation $\mathbf{n}$ except in terms involving the curvature $\partial\mathbf{u}/\partial s$. This approximation immediately reduces the forms of the orientational and tension stress to those found for a rigid rod. Terms involving the curvature $\partial\mathbf{u}/\partial s$ can be approximately by noting that $\partial\mathbf{u}/\partial s$ must be orthogonal to $\mathbf{u}$, because $\mathbf{u}(s)$ is a unit vector, and thus nearly orthogonal to $\mathbf{n}$: Approximating $\partial\mathbf{u}/\partial s$ by its projection onto the plane perpendicular to $\mathbf{n}$ yields $\partial\mathbf{u}/\partial s \simeq \partial^2\mathbf{h}/\partial s^2$. In this approximation

$$\boldsymbol{\sigma}_{\text{tens}} = c \int_0^L ds \langle \mathcal{T}\mathbf{nn}\rangle, \tag{73}$$

$$\boldsymbol{\sigma}_{\text{curv}} = c\kappa \int_0^L ds \left\langle \frac{\partial^2\mathbf{h}}{\partial s^2}\frac{\partial^2\mathbf{h}}{\partial s^2} - \mathbf{nn}\left|\frac{\partial^2\mathbf{h}}{\partial s^2}\right|^2 \right\rangle + \frac{ck_BTL}{a}\langle 3\mathbf{nn} - \mathbf{I}\rangle, \tag{74}$$

$$\boldsymbol{\sigma}_{\text{ornt}} = ck_BT\langle 3\mathbf{nn} - \mathbf{I}\rangle. \tag{75}$$

In Eqs. (73)–(75), $\langle\cdots\rangle$ represents a complete thermal average, over both the rapid fluctuations of $\mathbf{h}$, f, and $\mathcal{T}$, and over overall rod orientation $\mathbf{n}$. Below, we calculate $\boldsymbol{\sigma}_{\text{tens}}, \boldsymbol{\sigma}_{\text{curv}}$, and $\boldsymbol{\sigma}_{\text{ornt}}$ separately, and express $G(t)$ as a sum

$$G(t) = G_{\text{tens}}(t) + G_{\text{curv}}(t) + G_{\text{ornt}}(t) - \eta_s \delta(t), \tag{76}$$

of contributions arising from different stress contributions, where, e.g., $\boldsymbol{\sigma}_{\text{curv}}(t)$ $= G_{\text{curv}}(t)[\boldsymbol{\gamma}_0 + \boldsymbol{\gamma}_0^T]$, and similarly expand $G^*(\omega)$ and the intrinsic moduli $[G(t)]$ and $[G^*(\omega)]$.

VII. VISCOELASTICITY IN THE LCA

Here, the linear viscoelastic response of a solution of rods at intermediate and high frequencies, $\omega \gg \tau_\perp^{-1}$, is computed using the LCA for the average tension.

A. Tension stress

The LCA approximation for the tension stress is obtained by setting the tension in Eq. (73) equal to $\langle \mathcal{T}(s, \omega) \rangle = B(\omega)\langle \mathcal{E}(s, \omega) \rangle$, while using Eq. (58) for the strain. This yields a stress

$$\boldsymbol{\sigma}_{\text{tens}}(\omega) = cL \int_0^1 d\hat{s}\ B(\omega) \left\{ 1 - \frac{\cosh[\lambda(\omega)(\hat{s} - 1/2)]}{\cosh[\lambda(\omega)/2]} \right\} \boldsymbol{\gamma}(\omega) : \langle \mathbf{nnnn} \rangle. \tag{77}$$

Here, $\langle \cdots \rangle$ denotes an average over rod orientations, which can be approximated in a linear response calculation by an average over an isotropic distribution, using the identity [Doi and Edwards (1986)]:

$$\langle n_i n_j n_k n_l \rangle_{\text{eq}} = \tfrac{1}{15}(\delta_{ij}\delta_{kl} + \delta_{ik}\delta_{lj} + \delta_{il}\delta_{kj}) \tag{78}$$

for randomly oriented unit vectors. By evaluating the integral with respect to s, and requiring that the trace of $\boldsymbol{\gamma}(\omega)$ vanish in an incompressible fluid, we obtain a stress of the form

$$\boldsymbol{\sigma}_{\text{tens}}(\omega) = c[G^*_{\text{tens}}(\omega)][\boldsymbol{\gamma}(\omega) + \boldsymbol{\gamma}^T(\omega)], \tag{79}$$

with

$$[G^*_{\text{tens}}(\omega)] = \frac{1}{15}LB(\omega)\left\{ 1 - \frac{\tanh[\lambda(\omega)/2]}{\lambda(\omega)/2} \right\}. \tag{80}$$

Equation (80) has the following limiting behaviors

(1) *High frequencies and short times:* At frequencies $\omega \gg \tau_\parallel^{-1}$, for which $\lambda(\omega) \to \infty$, Eq. (80) reduces to

$$\lim_{\omega \gg \tau_\parallel^{-1}} [G^*_{\text{tens}}(\omega)] \simeq \frac{L}{15}B(\omega) \simeq \frac{2^{3/4}}{15}k_B T L L_p^2 \left(\frac{i\omega\zeta_\perp}{\kappa} \right)^{3/4}, \tag{81}$$

and hence, $[G^*_{\text{tens}}(\omega)] \propto \omega^{3/4}$. Inverse Fourier transforming this asymptote yields a modulus

$$\lim_{t \ll \tau_\parallel} [G_{\text{tens}}(t)] = C_1 k_B T L L_p^2 \left(\frac{\kappa t}{\zeta_\perp} \right)^{-3/4}, \tag{82}$$

where $C_1 = 2^{3/4}/[15\Gamma(\tfrac{1}{4})] = 0.0309$.

(2) *Intermediate frequencies and times:* At intermediate frequencies, such that $\tau_\parallel^{-1} \gg \omega \gg \tau_\perp^{-1}$, where $\lambda(\omega) = (i\omega\tau_\parallel)^{1/8} \ll 1$, Eq. (80) can be expanded in powers of $\lambda^2(\omega)$. The first two terms of the expansion are

$$[G_{\text{tens}}^*(\omega)] \simeq \frac{1}{180} i\omega\zeta_\parallel L^3 - \frac{k_B T}{1800\, 2^{3/4}} \left(\frac{\zeta_\parallel}{\zeta_\perp}\right)^2 (i\omega\tau_\perp)^{5/4} + \cdots. \tag{83}$$

The leading contribution, which arises from the leading order tension, is identical to the viscous contribution found for true rigid rods, and is purely imaginary. The first correction, which is proportional to $(i\omega)^{5/4}$, thus dominates the real part of $[G_{\text{tens}}^*(\omega)]$. We thus obtain a loss modulus $[G_{\text{tens}}''(\omega)] \propto \omega$, with the same prefactor as that of rigid rods, but a storage modulus $[G_{\text{tens}}'(\omega)] \propto \omega^{5/4}$. This $\omega^{5/4}$ contribution to $[G'(\omega)]$ is a subdominant contribution to $|[G^*]|$, because it is small compared to $[G''(\omega)]$, but is much larger than the ω-independent storage modulus of $\frac{3}{5}k_B T$ per chain found at these frequencies for rigid rods, and is found to dominate $[G'(\omega)]$.

Upon transforming this intermediate asymptote to the time domain, the leading order $i\omega$ term yields an apparent $\delta(t)$ contribution identical to that found for rigid rods, which does not contribute to $G(t)$ at intermediate times. As a result, $[G_{\text{tens}}(t)]$ is dominated at intermediate times by the transform of the $(i\omega)^{5/4}$ term, which yields

$$\lim_{\tau_\parallel \ll t \ll \tau_\perp} [G_{\text{tens}}(t)] \simeq C_2 k_B T \left(\frac{\zeta_\parallel}{\zeta_\perp}\right)^2 \left(\frac{t}{\tau_\perp}\right)^{-5/4}, \tag{84}$$

where $C_2 = 1/[2^{3/4} 7200 \Gamma(3/4)] = 6.74 \times 10^{-5}$. This stress arises from the $t^{-5/4}$ decay of the tension.

B. Curvature stress

Here, the curvature stress is computed with transverse equation of motion (24), in an approximation similar to that used to calculate the high-frequency compliance in Sec. IV, in which finite size effects are ignored and all quantities are expanded in a continuous distribution of Fourier modes.

We first expand Eq. (74) for the curvature stress in terms of Fourier amplitudes of h. Because $\boldsymbol{\sigma}_{\text{curv}}$ vanishes when the distribution of bending mode amplitudes is equilibrated [Morse (1998a)], the contribution of $\boldsymbol{\sigma}_{\text{curv}}$ from a rod with a specified orientation $\mathbf{n}$ may be equated with the difference between the rhs of Eq. (74) and its thermal equilibrium value. Expanding this difference in Fourier modes yields a contribution

$$\boldsymbol{\sigma}_{\text{curv}} = c\kappa \int \frac{dq}{2\pi} q^4 \langle \mathbf{b}(q,t) - \mathbf{n}\mathbf{n}\text{Tr}[\mathbf{b}(q,t)]\rangle_{\mathbf{n}}, \tag{85}$$

where $\mathbf{b}(q,t) \equiv \Sigma_{\alpha\beta} \mathbf{e}_\alpha(t)\mathbf{e}_\beta(t) b_{\alpha\beta}(q,t)$ is a tensor with components

$$b_{\alpha\beta}(q,t) \equiv \langle h_\alpha(q)h_\beta(-q)\rangle - \langle h_\alpha(q)h_\beta(-q)\rangle_{\text{eq}}. \tag{86}$$

Here, the average $\langle\cdots\rangle$ in Eq. (86) represents an average over fluctuations of the bending mode amplitudes for rods of known orientation, while the symbol $\langle\cdots\rangle_{\mathbf{n}}$ in Eq. (85) is used to indicate an average with respect to rod orientations.

To evaluate Eq. (85), it is convenient to calculate the contributions to $\mathbf{b}(q,t)$ and $\boldsymbol{\sigma}_{\text{curv}}$ that are induced by the presence of a nonzero value of $\dot{\gamma}_{\alpha\beta}$ in Eq. (38) separately from those induced by the existence of a nonzero tension and then add these two contributions.

(1) *Flow-induced curvature stress:* We first consider the contribution induced directly by the velocity gradient in Eq. (38), while setting $\mathcal{T} = 0$. The resulting contribution to $b_{\alpha\beta}(q,\omega)$ on a chain of known orientation in an oscillatory flow can be calculated using

equation of motion (38) by a method closely analogous to that used to derive Eq. (43) for $a(q,k;\omega)$ in Sec. IV. This yields

$$b_{\alpha\beta}(q,\omega) = \frac{k_B T L}{\kappa q^4} \frac{i\omega\zeta_\perp}{i\omega\zeta_\perp + 2\kappa q^4}[\gamma_{\alpha\beta}(\omega) + \gamma_{\beta\alpha}(\omega)]. \tag{87}$$

We then expand $\mathbf{b}(q,\omega) \equiv \Sigma_{\alpha\beta} b_{\alpha\beta}(q,\omega)\mathbf{e}_\alpha\mathbf{e}_\beta$, and use the identity $\Sigma_{\alpha\beta}\gamma_{\alpha\beta}(\omega)\mathbf{e}_\alpha\mathbf{e}_\beta = (\mathbf{I} - \mathbf{nn}) \cdot \boldsymbol{\gamma}(\omega) \cdot (\mathbf{I} - \mathbf{nn})$ to express $\mathbf{b}(q,\omega)$ explicitly as a function of $\boldsymbol{\gamma}(\omega)$ and $\mathbf{n}$. After substituting the resulting expression for $\mathbf{b}(q,\omega)$ into the temporal Fourier transform of Eq. (85), averaging over random rod orientations, and integrating with respect to q, we obtain a stress of the form $\boldsymbol{\sigma}_{\text{curv},t}(\omega) = c[G^*_{\text{curv,t}}][\boldsymbol{\gamma}(\omega) + \boldsymbol{\gamma}^T(\omega)]$, with an intrinsic modulus

$$[G^*_{\text{curv,t}}(\omega)] = \frac{3k_B T}{2^{3/4}10}(i\omega\tau_\perp)^{1/4}. \tag{88}$$

We refer to this as the "transverse" contribution to $[G^*_{\text{curv}}(\omega)]$, because it arises directly from the components of $\dot{\boldsymbol{\gamma}}(\omega)$ along the directions transverse to $\mathbf{n}$.

(2) *Tension-induced curvature stress:* We next consider the contribution to $\mathbf{b}(q,\omega)$ and $\boldsymbol{\sigma}_{\text{curv}}(\omega)$ induced by the tension on the rhs of Eq. (38), while setting $\dot{\gamma}_{\alpha\beta} = 0$. This calculation is closely analogous to the calculation of $a(q,k;\omega)$ in the case $k = 0$. On an infinite chain, $b_{\alpha\beta}(q,\omega)$ depends only on the $q = 0$ component of the tension, as a result of translational invariance. On a finite chain at intermediate or high frequencies, $b_{\alpha\beta}(q,\omega)$ thus depends upon the integral $\mathcal{T}(q = 0,\omega) = \int ds\, \mathcal{T}(s,\omega)$. Another calculation analogous to that leading to Eq. (43), in which the tension in Eq. (38) is equated to the thermal average $\langle \mathcal{T}(s,\omega)\rangle$, yields

$$b_{\alpha\beta}(q,\omega) = -\delta_{\alpha\beta}\frac{2k_B T}{\kappa q^2}\frac{1}{i\omega\zeta_\perp + 2\kappa q^4}\int_0^L ds\, \langle\mathcal{T}(s,\omega;\mathbf{n})\rangle, \tag{89}$$

in which $\langle\mathcal{T}(s,\omega;\mathbf{n})\rangle$ is the average, with respect to rapid transverse fluctuations of the tension in a rod with known orientation $\mathbf{n}$. Substituting this expression into Eq. (85), and again evaluating averages with respect to chain orientations using Eq. (78), yields a stress contribution characterized by an intrinsic modulus

$$[G^*_{\text{curv,l}}(\omega)] = \frac{3}{2^{5/4}}\frac{L}{L_p}(i\omega\tau_\perp)^{-1/4}[G^*_{\text{tens}}(\omega)]. \tag{90}$$

Here $[G^*_{\text{tens}}(\omega)]$ is the tension modulus given in Eq. (80), which also depends on the integral $\int ds\langle\mathcal{T}(s,\omega;\mathbf{n})\rangle$. Equation (90) has the following limiting behaviors: For $\omega \gg \tau_\parallel^{-1}$, where $[G^*_{\text{tens}}(\omega)] \propto (i\omega)^{3/4}$,

$$\lim_{\omega \gg \tau_\parallel^{-1}} [G^*_{\text{curv,l}}(\omega)] \sim k_B T\left(\frac{L_p}{L}\right)(i\omega\tau_\perp)^{1/2}. \tag{91}$$

For $\tau_\parallel^{-1} \gg \omega \gg \tau_\perp^{-1}$, where the dominant contribution to $[G^*_{\text{tens}}]$ scales as $(k_B T L_p/L)(i\omega\tau_\perp)$,

$$\lim_{\tau_\parallel^{-1} \gg \omega \gg \tau_\perp^{-1}} [G^*_{\text{curv,l}}(\omega)] \sim k_B T\frac{\zeta_\parallel}{\zeta_\perp}(i\omega\tau_\perp)^{3/4}. \tag{92}$$

$[G^*_{\text{curv,l}}(\omega)]$ is termed the "longitudinal" contribution to $[G^*_{\text{curv}}(\omega)]$ because it arises from the tension, which is proportional to the component $\dot{\gamma}(\omega){:}\mathbf{nn}$ of $\dot{\gamma}$ along $\mathbf{n}$. The total curvature modulus $[G^*_{\text{curv}}(\omega)]$ is given by the sum of $[G^*_{\text{curv,}t}(\omega)]$ and $[G^*_{\text{curv,}l}(\omega)]$.

C. Results

The total modulus is given by the sum of the tension and curvature contributions calculated earlier and of an orientational contribution. In the rodlike limit, $L \ll L_p$, the orientational contribution can be approximated by that of a dilute solution of rigid rods

$$[G^*_{\text{ornt}}(\omega)] = \frac{3}{5}k_B T \frac{i\omega\tau_{\text{rod}}}{1 + i\omega\tau_{\text{rod}}}. \tag{93}$$

For frequencies $\omega\tau_{\text{rod}} \gg 1$, this expression for $[G^*_{\text{ornt}}]$ yields a plateau of magnitude $\frac{3}{5}k_B T$ in the storage modulus.

This orientational component dominates the total storage modulus at low frequencies, $\omega \ll \tau_\perp^{-1}$, giving behavior identical to that of rigid rods, but becomes negligible compared to either the tension or curvature components at intermediate and high frequencies. A comparison of the earlier expressions for the different contributions to $G^*(\omega)$ shows that, throughout intermediate and high frequency regimes, they form a hierarchy

$$G^*_{\text{ornt}}(\omega) \ll G^*_{\text{curv,}t}(\omega) \ll G^*_{\text{curv,}l}(\omega) \ll G^*_{\text{tens}}(\omega). \tag{94}$$

The tension contribution $[G^*_{\text{tens}}(\omega)]$ dominates the total modulus at all $\omega \gg \tau_\perp^{-1}$. At frequencies $\omega \sim \tau_\perp^{-1}$, all four of these contributions to $[G^*(\omega)]$ become comparable to $k_B T$, and thus to each other. Though the earlier LCA calculation is valid only at $\omega \gg \tau_\perp^{-1}$, the more complete calculation given in the next section shows that both the curvature and tension contributions to $G(t)$ decay exponentially at $t \gg \tau_\perp$, with terminal times of order $\tau_\perp$, leading to terminal behavior in the corresponding components of $G^*(\omega)$ at $\omega \ll \tau_\perp^{-1}$. The resulting time dependence of $G_{\text{tens}}(t), G_{\text{curv}}(t)$, and $G_{\text{ornt}}(t)$ for chains with $L \ll L_p$ is shown schematically in Fig. 2.

VIII. FULL THEORY

In order to describe accurately viscoelasticity at frequencies of order $\tau_\perp^{-1}$ and lower, the preceding calculation must be extended in two ways. First, because the nonlocality of $\chi(s,s';\omega)$ becomes important at these frequencies, we must abandon the LCA and use the full nonlocal compliance when solving the average longitudinal force balance of Eq. (30), while respecting the condition that the tension vanish at both chain ends. Second, when using the transverse equation of motion to calculate both the compliance and the curvature stress, the transverse displacement field must be expanded in discrete eigenmodes that respect the boundary conditions for the transverse dynamics. To formulate a full theory, accurate at arbitrary frequency, we first introduce expansions of $\mathcal{T}$ and h in appropriate basis functions.
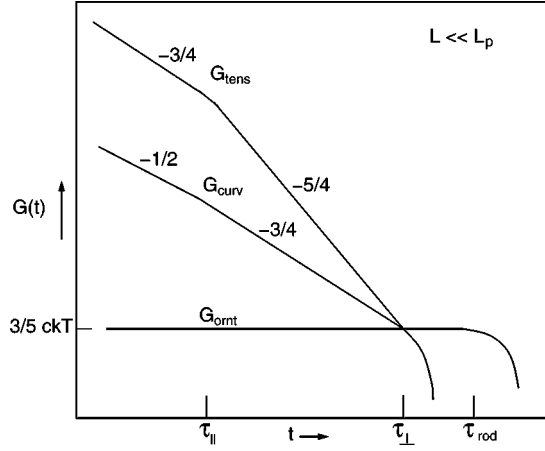
FIG. 2. Schematic showing the asymptotic behaviors of $G_{\text{tens}}(t), G_{\text{curv}}(t)$, and $G_{\text{ornt}}(t)$, in a log–log plot, for stiff chains with $L \ll L_p$.

A. Longitudinal mode expansion

The tension $\mathcal{T}(\hat{s})$, which must vanish at both ends of the chain, is expanded in a basis of sines

$$\mathcal{T}(\hat{s}) = \sum_k \mathcal{T}_k \phi_k(\hat{s}), \quad \phi_k(\hat{s}) = \sqrt{2}\sin(\lambda_k \hat{s}), \tag{95}$$

where $\lambda_k = k\pi$ for $k = 1,2,3,\dots$. Substituting this expansion into Eq. (30), multiplying the result by $\phi_i(\hat{s})$ and integrating with respect to $\hat{s}$ yields the expansion of the longitudinal force balance

$$\sum_k \left[i\omega\zeta_\parallel \chi_{ik}(\omega) + \frac{\kappa}{L^4}\left[\frac{\partial^4 \chi(\omega)}{\partial \hat{s}^4}\right]_{ik} + \delta_{ik}\frac{\lambda_i^2}{L^2}\right]\langle \mathcal{T}_k \rangle = i\omega\zeta_\parallel \boldsymbol{\gamma}(\omega):\mathbf{nn}\mathcal{F}_i, \tag{96}$$

where

$$\chi_{ik}(\omega) = L\int_0^1 d\hat{s}\int_0^1 ds'\,\phi_i(\hat{s})\phi_k(\hat{s}')\chi(\hat{s},\hat{s}';\omega), \tag{97}$$

$$\left[\frac{\partial^4 \chi(\omega)}{\partial \hat{s}^4}\right]_{ik} = L\int_0^1 d\hat{s}\int_0^1 d\hat{s}'\,\phi_i(\hat{s})\frac{\partial^4}{\partial \hat{s}^4}\chi(\hat{s},\hat{s}';\omega), \tag{98}$$

and

$$\mathcal{F}_i = \int_0^1 d\hat{s}\,\phi_i(\hat{s}) = \begin{cases} \dfrac{2\sqrt{2}}{i\pi} & i \text{ odd} \\ 0 & i \text{ even} \end{cases}. \tag{99}$$

Here, $\chi_{ik}(\omega)$ are the ''matrix elements'' of $\chi(s,s';\omega)$ in a basis of sines.

B. Transverse mode expansion

The transverse displacement $h_\alpha(\hat{s})$ is expanded as

$$h_\alpha(\hat{s}) = \sum_j \tilde{h}_{\alpha,j} \mathcal{W}_j(\hat{s}), \tag{100}$$

where $\mathcal{W}_j$ is the jth normalized eigenfunction of the fourth order eigenvalue problem [Aragon and Pecora (1985), Kroy and Frey (1997), Wiggins *et al.* (1998)]:

$$\frac{\partial^4 \mathcal{W}_j(\hat{s})}{\partial \hat{s}^4} = \alpha_j^4 \mathcal{W}_j(\hat{s}), \tag{101}$$

subject to the homogeneous boundary conditions

$$\frac{\partial^2 \mathcal{W}_j}{\partial \hat{s}^2} = \frac{\partial^3 \mathcal{W}_j}{\partial \hat{s}^3} = 0 \tag{102}$$

at $\hat{s} = 0$ and $\hat{s} = 1$. The eigenfunctions $\mathcal{W}_j$ are orthogonal, because the differential operator in (101) is self-adjoint, and are taken to be orthonormal, so that $\int_0^1 d\hat{s} \mathcal{W}_j \mathcal{W}_k = \delta_{jk}$. The eigenvalue problem has a degenerate trivial eigenvalue $\alpha_0 = 0$, with eigenfunctions $\mathcal{W} = 1$ and $\mathcal{W} = \sqrt{12}(\hat{s} - 1/2)$ corresponding to rigid translations and rotations, respectively. The nontrivial eigenfunctions, corresponding to bending modes, are

$$\mathcal{W}_j(\hat{s}) = A_j\{[\sinh(\alpha_j) + \sin(\alpha_j)][\sin(\alpha_j\hat{s}) + \sinh(\alpha_j\hat{s})]$$
$$+ [\cos(\alpha_j) - \cosh(\alpha_j)][\cos(\alpha_j\hat{s}) + \cosh(\alpha_j\hat{s})]\}, \tag{103}$$

where $A_j = [\frac{1}{2} + \frac{1}{2}\cosh(2\alpha_j) + \alpha_j^{-1}\cosh(\alpha_j)\sin(\alpha_j)]^{-1/2}$. The eigenvalues α_j satisfy the solvability condition $\cos(\alpha_j) = 1/\cosh(\alpha_j)$. The first few nontrivial eigenvalues are $\alpha_1 = 4.73 = 3\pi/2 + 0.0176$, $\alpha_2 = 5\pi/2 - 0.000\,781\,6$, and $\alpha_3 = 7\pi/2 + 0.000\,033\,5$. Higher eigenvalues are accurately approximated by setting $\cos(\alpha_j) = 0$, which yields $\alpha_j = (2j+1)\pi/2$.

The harmonic approximation (37) of the bending energy can be expanded in mode amplitudes as

$$U_{\text{bend}} = \frac{1}{2}\frac{\kappa}{L^3} \sum_j \alpha_j^4 (\tilde{h}_{\alpha,j})^2. \tag{104}$$

The transverse dynamical Eq. (24) can be expanded by substituting expansion (100) for h_α and expansion (95) for $\mathcal{T}$, multiplying the result by $\mathcal{W}_j(s)$, and integrating with respect to s; this yields

$$\zeta_\perp \sum_\beta \left[\delta_{\alpha\beta}\frac{\partial}{\partial t} - \dot{\gamma}_{\alpha\beta}\right]\tilde{h}_{\beta,j} = -\kappa L^{-4}\alpha_j^4\tilde{h}_{\alpha,j} - \frac{1}{L^2}\sum_{lk} H_{ljk}\mathcal{T}_l\tilde{h}_{\alpha,k} + \tilde{\eta}_{\alpha,j}, \tag{105}$$

where

$$H_{ljk} \equiv \int_0^1 d\hat{s}\, \phi_l(\hat{s})\frac{\partial \mathcal{W}_j(\hat{s})}{\partial \hat{s}}\frac{\partial \mathcal{W}_k(\hat{s})}{\partial \hat{s}}, \tag{106}$$

and $\tilde{\eta}_{\alpha,j} = \int_0^L d\hat{s}\mathcal{W}_j(\hat{s})\eta_\alpha(\hat{s})$ is a mode amplitude for component α of the transverse noise $\boldsymbol{\eta}_\perp$.

C. Nonlocal compliance

We now present a calculation of the nonlocal compliance $\chi(s,s';\omega)$ at arbitrary frequency. The longitudinal strain given in Eq. (23) is expanded as

$$\langle \mathcal{E}(\hat{s}) \rangle = -\frac{1}{L^2} \sum_{jm} \frac{\partial \mathcal{W}_j}{\partial \hat{s}} \frac{\partial \mathcal{W}_m}{\partial \hat{s}} a_{jm}, \tag{107}$$

where

$$a_{jm} \equiv \frac{1}{2} \sum_{\alpha} [\langle \tilde{h}_{\alpha,j} \tilde{h}_{\alpha,m} \rangle - \langle \tilde{h}_{\alpha,j} \tilde{h}_{\alpha,m} \rangle_{\text{eq}}]. \tag{108}$$

To calculate the compliance, we derive an expression for $da_{jm}(t)/dt$ in the presence of an infinitesimal tension, while setting $\gamma_{\alpha\beta}(\omega) = 0$, by a method closely analogous to that used to derive Eq. (42) for $da(q,k;t)/dt$. Here, we use expansion (105) of the transverse dynamical equation, and evaluate the required thermal averages using the relations $\langle \tilde{h}_{\alpha,j} \tilde{h}_{\beta,k} \rangle_{\text{eq}} = \delta_{\alpha\beta} \delta_{kj} k_B T L^3/(\kappa \alpha_k^4)$ and $\langle \tilde{\eta}_{\alpha,j} \tilde{h}_{\beta,k} \rangle = \delta_{\alpha\beta} \delta_{jk} k_B T/L$. This yields the differential equation

$$\left\{ \zeta_\perp \frac{\partial}{\partial t} + \kappa L^{-4}(\alpha_j^4 + \alpha_m^4) \right\} a_{jm}(t) = -\frac{k_B T L}{\kappa} (\alpha_m^{-4} + \alpha_j^{-4}) \sum_l H_{lmj} \mathcal{T}_l(t), \tag{109}$$

for $a_{jm}(t)$, or the equivalent algebraic equation

$$a_{jm}(\omega) = -\frac{k_B T L}{\kappa} \frac{\alpha_m^{-4} + \alpha_j^{-4}}{i\omega\zeta_\perp + \kappa L^{-4}(\alpha_j^4 + \alpha_m^4)} \sum_l H_{lmj} \mathcal{T}_l(\omega), \tag{110}$$

for its Fourier transform $a_{jm}(\omega) \equiv \int dt\, a_{jm}(t) e^{-i\omega t}$. Substituting Eq. (110) for $a_{jm}(\omega)$ into Eq. (107) yields an average strain of the form $\langle \mathcal{E}(s,\omega) \rangle = \int_0^L ds' \chi(s,s';\omega) \mathcal{T}(s',\omega)$, where

$$\chi(s,s';\omega) = \frac{k_B T}{\kappa L^2} \sum_{ljm} \frac{(\alpha_m^{-4} + \alpha_j^{-4}) H_{ljm}}{i\omega\zeta_\perp + \kappa L^{-4}(\alpha_j^4 + \alpha_m^4)} \frac{\partial \mathcal{W}_j(\hat{s})}{\partial \hat{s}} \frac{\partial \mathcal{W}_m(\hat{s})}{\partial \hat{s}} \phi_l(\hat{s}') \tag{111}$$

is the desired nonlocal compliance.

The matrix elements $\chi_{ik}(\omega)$ and $[\partial^4 \chi/\partial s^4]_{jk}$ defined in Eqs. (97) and (98) can be obtained by evaluating the defining double integral, using the orthonormality of the functions $\phi_k(\hat{s})$. The result can be expressed in terms of non-dimensional matrix elements $\bar{\chi}_{ik}(\omega) \equiv i\omega\zeta_\perp L^2 \chi_{ik}(\omega)$ and $[\partial^4 \bar{\chi}/\partial \hat{s}^4]_{ik} \equiv i\omega\zeta_\perp L^2 [\partial^4 \chi(\omega)/\partial \hat{s}^4]_{ik}$, which are given by

$$\bar{\chi}_{ik}(\omega) = \frac{L}{L_p} \sum_{jm} \frac{(\alpha_j^{-4} + \alpha_m^{-4}) H_{ijm} H_{kjm}}{1 + (i\omega\tau_\perp)^{-1}(\alpha_j^4 + \alpha_m^4)}, \tag{112}$$

$$\left[\frac{\partial^4 \bar{\chi}(\omega)}{\partial \hat{s}^4} \right]_{ik} = \frac{L}{L_p} \sum_{j,m} \frac{(\alpha_j^{-4} + \alpha_m^{-4}) F_{ijm} H_{kjm}}{1 + (i\omega\tau_\perp)^{-1}(\alpha_j^4 + \alpha_m^4)}, \tag{113}$$

where

$$F_{ijm} = \int_0^1 d\hat{s}\, \phi_i \frac{\partial^4}{\partial \hat{s}^4} \left(\frac{\partial \mathcal{W}_j}{\partial \hat{s}} \frac{\partial \mathcal{W}_m}{\partial \hat{s}} \right).$$

D. Tension and tension stress

To calculate the spatial Fourier components of the average tension, longitudinal force balance (96) can be expressed in nondimensional form as a matrix equation

$$\sum_k \left\{ \frac{\zeta_\parallel}{\zeta_\perp} \bar{\chi}_{ik}(\omega) + \frac{1}{i\omega\tau_\perp} \left[\frac{\partial^4 \bar{\chi}(\omega)}{\partial \hat{s}^4} \right]_{ik} + \lambda_i^2 \delta_{ik} \right\} \langle T_k^*(\omega) \rangle = \mathcal{F}_i, \tag{114}$$

where

$$\langle T_k^*(\omega) \rangle \equiv \frac{\langle \mathcal{T}_k(\omega;\mathbf{n}) \rangle}{i\omega\zeta_\parallel L^2 \boldsymbol{\gamma}(\omega):\mathbf{nn}} \tag{115}$$

is the nondimensional Fourier component of the tension, and $\langle \mathcal{T}_k(\omega;\mathbf{n}) \rangle$ is a Fourier amplitude for the average tension in a chain with a known orientation $\mathbf{n}$. By Eq. (96), $\langle \mathcal{T}_k(\omega;\mathbf{n}) \rangle$ depends linearly on $\boldsymbol{\gamma}(\omega):\mathbf{nn}$. This dependence has been factored out in the earlier definition, so that the reduced Fourier amplitude $\langle T_k^*(\omega) \rangle$ is independent of both $\mathbf{n}$ and $\boldsymbol{\gamma}(\omega)$. These reduced Fourier amplitudes are calculated by solving matrix Eq. (114) with a finite number of modes.

The tension modulus $G_{\text{tens}}^*(\omega)$ is calculated by substituting expansion (95) in Eq. (73) for the tension stress, while using Eq. (115) to recast the results in terms of the dimensionless Fourier components of the tension. This yields a stress

$$\boldsymbol{\sigma}_{\text{tens}}(\omega) = c i\omega\zeta_\parallel L^3 \boldsymbol{\gamma}(\omega):\langle\mathbf{nnnn}\rangle \sum_p \langle T_p^*(\omega) \rangle \mathcal{F}_p. \tag{116}$$

After evaluating the average of $\langle\mathbf{nnnn}\rangle$ over rod orientations, as before, we obtain a stress of the form $\boldsymbol{\sigma}_{\text{tens}}(\omega) = c[G_{\text{tens}}^*(\omega)][\boldsymbol{\gamma}(\omega) + \boldsymbol{\gamma}^T(\omega)]$, with

$$[G_{\text{tens}}^*(\omega)] = \tfrac{1}{15} i\omega\zeta_\parallel L^3 \sum_p \langle T_p^*(\omega) \rangle \mathcal{F}_p. \tag{117}$$

E. Curvature stress

Substituting expansion (100) for the transverse displacement in Eq. (74) for the curvature stress, and using the fact that $\boldsymbol{\sigma}_{\text{curv}}$ vanishes when the bending modes are equilibrated, yields an expansion of the curvature stress as

$$\sigma_{\text{curv}} = c\kappa L^{-3} \sum_k \alpha_k^4 \langle \mathbf{b}_k - \mathbf{nn} \operatorname{Tr}[\mathbf{b}_k] \rangle_{\mathbf{n}}, \tag{118}$$

where $\mathbf{b}_k(t) \equiv \sum_{\alpha\beta} \mathbf{e}_\alpha(t) \mathbf{e}_\beta(t) b_{k,\alpha\beta}(t)$ is a tensor with components

$$b_{k,\alpha\beta} \equiv \langle h_{\alpha,k} h_{\beta,k} \rangle - \langle h_{\alpha,k} h_{\beta,k} \rangle_{\text{eq}}. \tag{119}$$

The calculation of the components of $\mathbf{b}_k(\omega)$ in a weak oscillatory flow field is closely analogous to the calculation of $\mathbf{b}(q,\omega)$ given in Sec. VII B, except for the use of expansions (100) and (95) for h and $\mathcal{T}$, respectively, rather than Fourier transforms, and the corresponding use of Eq. (105) for time derivatives of the mode amplitudes. As in Sec. VII B, we consider separately the contributions to $\mathbf{b}_k$ and $\boldsymbol{\sigma}_{\text{curv}}$ arising from the direct coupling of the velocity gradient to h, and from the tension.

(1) *Flow-induced curvature stress:* We calculate the curvature stress that is induced directly by the velocity gradient tensor by calculating the time derivative of $b_{k,\alpha\beta}(t)$, which setting the tension to zero in Eq. (105). This yields

$$b_{k,\alpha\beta}(\omega) = \frac{k_B T L^3}{\kappa \alpha_k^4} \frac{i\omega\zeta_\perp}{i\omega\zeta_\perp + 2\kappa L^{-4}\alpha_k^4} [\gamma_{\alpha\beta}(\omega) + \gamma_{\beta\alpha}(\omega)] \tag{120}$$

for the Fourier transform of $b_{k,\alpha\beta}(t)$. Substituting Eq. (120) in Eq. (118), and evaluating the orientational averages yields a stress contribution $\boldsymbol{\sigma}_{\mathrm{curv,t}}(\omega) = c[G^*_{\mathrm{curv}}(\omega)][\boldsymbol{\gamma}(\omega) + \boldsymbol{\gamma}^T(\omega)]$, with

$$[G^*_{\mathrm{curv,t}}(\omega)] = \frac{3}{5}k_B T \sum_k \frac{i\omega\zeta_\perp}{i\omega\zeta_\perp + 2\kappa L^{-4}\alpha_k^4}. \tag{121}$$

(2) *Tension-induced curvature stress:* The contribution to $b_{k,\alpha\beta}$ induced by the tension, for $\boldsymbol{\gamma}(\omega) = 0$, is given by

$$b_{k,\alpha\beta} = -\delta_{\alpha\beta} \frac{2k_B T L}{\kappa\alpha_k^4} \frac{1}{i\omega\zeta_\perp + 2\kappa\alpha_k^4 L^{-4}} \sum_l H_{lkk}\langle \mathcal{T}_l(\omega)\rangle. \tag{122}$$

Substituting this in Eq. (118), expressing the tension coefficients in terms of the reduced coefficients $\langle \mathcal{T}^*(\omega)\rangle$, and averaging over chain orientations, yields a stress contribution characterized by an intrinsic modulus

$$[G^*_{\mathrm{curv,l}}(\omega)] = \frac{2}{5}k_B T \sum_k \frac{i\omega\zeta_\parallel}{i\omega\zeta_\perp + 2\kappa L^{-4}\alpha_k^4} \sum_l H_{lkk}\langle \mathcal{T}^*_l(\omega)\rangle. \tag{123}$$

F. Results

The total complex modulus of dilute solutions of semiflexible rods, with $L \ll L_p$ but arbitrary frequency, is obtained by adding Eqs. (117), (121), (123), and (93):

$$\begin{aligned}
\frac{[G^*(\omega)]}{k_B T} &= \frac{24}{5}\frac{\zeta_\parallel}{\zeta_\perp}(i\omega\tau_{\mathrm{rod}})\sum_k \langle \mathcal{T}^*_k(\omega)\rangle \mathcal{F}_k \\
&\quad + \frac{2}{5}\frac{\zeta_\parallel}{\zeta_\perp}\sum_k \frac{1}{1+2\alpha_k^4(i\omega\tau_\perp)^{-1}} \sum_l \langle \mathcal{T}^*_l(\omega)\rangle H_{lkk} \\
&\quad + \frac{3}{5}\sum_k \frac{1}{1+2\alpha_k^4(i\omega\tau_\perp)^{-1}} \\
&\quad + \frac{3}{5}\frac{i\omega\tau_{\mathrm{rod}}}{1+i\omega\tau_{\mathrm{rod}}},
\end{aligned} \tag{124}$$

where $\langle \mathcal{T}^*_k\rangle$ is obtained as a solution to matrix Eq. (114), $\mathcal{F}_k$ is defined in Eq. (99), and H_{ljm} is defined in Eq. (106). The first line in Eq. (124) represents $[G^*_{\mathrm{tens}}(\omega)]$, the second line represents $[G^*_{\mathrm{curv,l}}(\omega)]$ the third $[G^*_{\mathrm{curv,t}}]$, and the fourth $[G^*_{\mathrm{ornt}}(\omega)]$.

An example of theoretical predictions for various contributions to the storage and loss modulus, viz. $[G^*_{\mathrm{tens}}]$, $[G^*_{\mathrm{curv,l}}]$, $[G^*_{\mathrm{curv,t}}]$, and $[G^*_{\mathrm{ornt}}]$, are shown in Fig. 3 for $L/L_p = 1/8$. Also plotted in this figure are the corresponding asymptotes derived in Sec. VII for high and intermediate frequency regimes. Note that the high frequency $\omega^{3/4}$ asymptotes of $[G'(\omega)]$ and $[G''(\omega)]$ are approached rather slowly and at very high frequen-
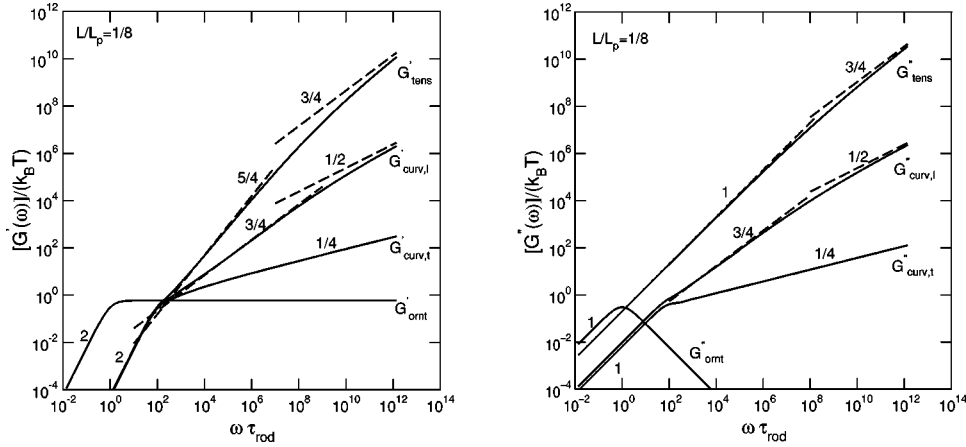
FIG. 3. Predictions of the full theory for the tension (tens), curvature, (curv,*l* and curv,*t*), and orientation (ornt) contributions to the intrinsic storage modulus $[G'(\omega)]$ (left panel) and intrinsic loss modulus $[G''(\omega)]$ (right panel), divided by $k_B T$, as functions of $\omega\tau_{\text{rod}}$ for $L/L_p = 1/8$. Intrinsic moduli are defined in Eq. (12) as contributions per chain. Dashed lines are the asymptotic power laws predicted for each component at intermediate and high frequencies.

cies, $\omega\tau_{\text{rod}} \gg 10^9$, corresponding roughly to $\omega \gg \tau_\parallel^{-1}$. The slow approach to this asymptote is a result of the slow $\omega^{-1/8}$ decrease in the thickness of the boundary layers at the chain ends. The $\omega^{5/4}$ dependence of $[G'_{\text{tens}}(\omega)]$ at intermediate frequencies is clearly visible for this value of L/L_p, over a range $\omega\tau_{\text{rod}} \sim 10^3$–$10^6$. The quantity $[G''_{\text{tens}}(\omega)]$, which dominates $[G''(\omega)]$ at all $\omega \gg \tau_{\text{rod}}^{-1}$, is proportional to ω at all $\omega \ll \tau_\parallel^{-1}$, with a constant of proportionality identical to that found for rigid rods. As a result, $[G''(\omega)]$ for a solution of semiflexible rods closely approaches that of a corresponding rigid rod solution at all $\omega \ll \tau_\parallel^{-1}$. Both the tension contribution and the two curvature contributions to $[G^*(\omega)]$ exhibit terminal behavior below $\omega\tau_{\text{rod}} \sim 10^2$, corresponding roughly to frequencies below the relaxation rate $\alpha_1^4 \tau_\perp^{-1}$ of the longest wavelength bending mode. At all lower frequencies, for which the bending modes are relaxed, the overall $[G'(\omega)]$ and $[G''(\omega)]$ both closely mimic the behavior of rigid rods, leading to a plateau of magnitude $[G'(\omega)] = \frac{3}{5}k_B T$ at $\tau_{\text{rod}} < \omega < \alpha_1^4 \tau_\perp^{-1}$, which grows broader as L/L_p is decreased, and terminal behavior at $\omega \ll \tau_{\text{rod}}^{-1}$.

Figure 4 shows the evolution of the total predicted storage and loss moduli as L/L_p is varied from 1/8 to 1. As L/L_p increases, both the $\omega^{5/4}$ intermediate regime in $G'(\omega)$ and the orientational plateau at lower frequencies gradually disappear, while the high-frequency $\omega^{3/4}$ asymptote is approached at lower reduced frequencies for more flexible chains.

Figure 5 compares the predictions of the full theory to those of the LCA, and to the analytic approximation of Sec. XI, for $L/L_p = 1/8$. The LCA agrees well with the full theory at frequencies well above the relaxation rate $\alpha_1^4 \tau_\perp^{-1}$ of the longest wavelength bending mode, but fails at lower frequencies. The conspicuous failure of the LCA at low frequencies is primarily a result of the fact that the LCA predicts algebraic frequency and time dependence for the tension and curvature contributions to the modulus even at frequencies $\omega < \tau_\perp^{-1}$, due to the use of a continuous distribution of modes with no lower cutoff, which yields a theory with no terminal relaxation time. The full theory instead
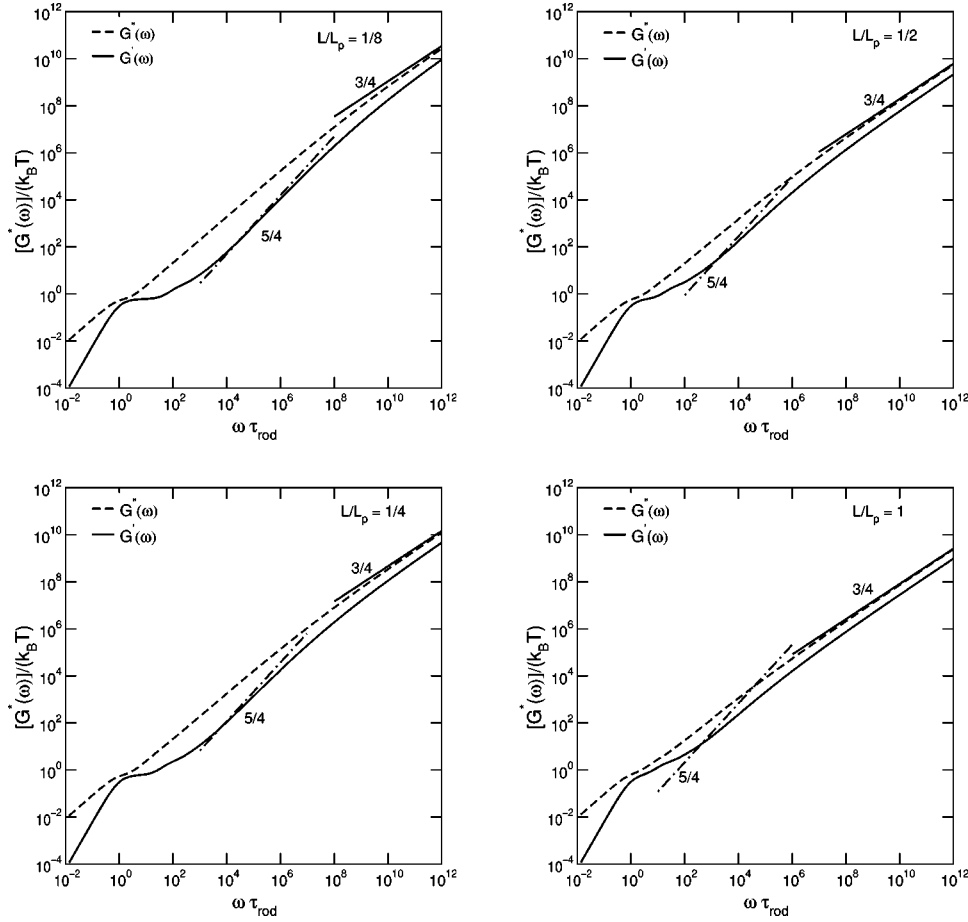
FIG. 4. The storage $[G'(\omega)]$ and loss $[G''(\omega)]$ moduli vs $\omega\tau_{\mathrm{rod}}$ obtained from the full theory for different values of L/L_p. The solid and dash-dotted straight lines are the predicted $\omega^{3/4}$ high-frequency asymptote for G'' and $\omega^{5/4}$ intermediate frequency asymptote for G', respectively.

yields normal terminal frequency dependence of all components of $G^*(\omega)$ at these frequencies, and exponential decay in $G(t)$ at corresponding times, due to the finite length of the chain. Because existing experimental data for dilute solutions of semiflexible rods (which are discussed in Sec. X) are in the regime $\omega\tau_{\mathrm{rod}} < 10^4$, we must use the full theory when making quantitative comparisons to experiments.

IX. BROWNIAN DYNAMICS SIMULATIONS

To test these predictions over a much wider frequency range than those accessible to current experiments, we have carried out Brownian dynamics simulations of noninteracting, free-draining wormlike chains. We simulate discretized wormlike chains in which each chain contains N beads with positions $\mathbf{R}_i$ for $i = 1,...,N$, which act as point sources of frictional resistance, connected by $N-1$ rods of constant length a. We use a discretized bending energy

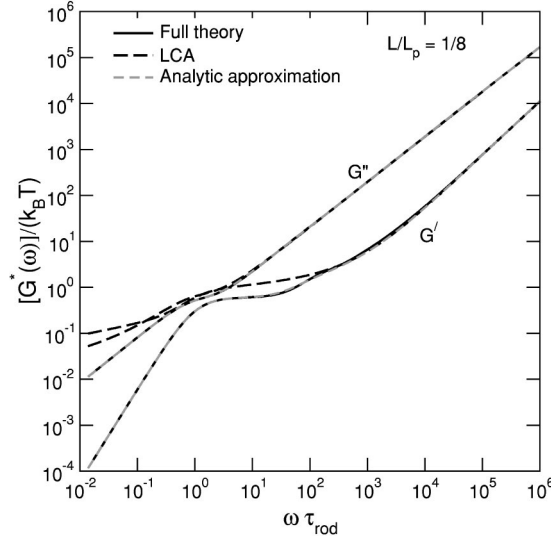**FIG. 5.** Comparison of predictions for $G'(\omega)$) and $G''(\omega)$ as functions of $\omega\tau_{\mathrm{rod}}$ for $L/L_p = 1/8$, as obtained from the full theory (continuous black lines), the local compliance approximation (dashed black lines), and the analytic approximation of Sec. XI (dashed gray lines).

$$U_{\mathrm{bend}} = -\frac{\kappa}{a}\sum_{i=2}^{N-1}\mathbf{u}_i\cdot\mathbf{u}_{i-1}, \tag{125}$$

where

$$\mathbf{u}_i \equiv \frac{\mathbf{R}_{i+1}-\mathbf{R}_i}{|\mathbf{R}_{i+1}-\mathbf{R}_i|} \tag{126}$$

is a unit tangent vector along rod i. For simplicity, we simulate free-draining chains with isotropic friction at each bead, corresponding to a continuum model with $\zeta_\| = \zeta_\perp = \zeta$, in the creeping flow limit, where we ignore any inertia of the chain.

The equation of motion for a chain in a flow with velocity gradient $\dot{\boldsymbol{\gamma}}$ is

$$\zeta_b\left[\frac{d\mathbf{R}_i}{dt} - \dot{\boldsymbol{\gamma}}\cdot\mathbf{R}_i\right] = \mathbf{F}_i = \mathbf{F}_i^{\mathrm{bend}} + \mathbf{F}_i^{\mathrm{met}} + \mathbf{F}_i^{\mathrm{tens}} + \mathbf{F}_i^{\mathrm{rand}}. \tag{127}$$

Here, $\zeta_b = \zeta a$ is a bead friction coefficient, $\mathbf{F}_i^{\mathrm{bend}} = -\partial U_{\mathrm{bend}}/\partial\mathbf{R}_i$ is the force on bead i due to the bending of the chain, $\mathbf{F}_i^{\mathrm{met}}$ is a "metric force" (discussed below), $\mathbf{F}_i^{\mathrm{tens}}$ is a constraint force that is chosen to impose the constraints of constant rod length (discussed below), and $\mathbf{F}_i^{\mathrm{rand}}$ is a random Langevin force with vanishing mean and a variance $\langle\mathbf{F}_i^{\mathrm{rand}}(t)\mathbf{F}_j^{\mathrm{rand}}(t')\rangle = 2k_BT\zeta_b\mathbf{I}\delta_{ij}\delta(t-t')$ given by the fluctuation dissipation theorem. The stochastic equation of motion (127) for the bead positions $\mathbf{R}_i$ is integrated numerically with a mid-step algorithm [Grassia and Hinch (1996)] to generate bead trajectories.

The constraint force $\mathbf{F}_i^{\mathrm{tens}}$ is of the form

$$\mathbf{F}_i^{\mathrm{tens}} \equiv \mathcal{T}_i\mathbf{u}_i - \mathcal{T}_{i-1}\mathbf{u}_{i-1}, \tag{128}$$

where $\mathcal{T}_i$ is the tension in bond i. Requiring that $\frac{d}{dt}|\mathbf{R}_{i+1} - \mathbf{R}_i|^2 = 0$ for each bond in the chain, and using Eq. (127) to calculate this time derivative, yields a set of linear equations for the instantaneous tensions

$$\sum_{j=1}^{N-1} H_{ij}\mathcal{T}_j = \mathbf{u}_i \cdot (\tilde{\mathbf{F}}_{i+1} - \tilde{\mathbf{F}}_i), \tag{129}$$

where $\tilde{\mathbf{F}}_i \equiv \mathbf{F}_i^{\text{bend}} + \mathbf{F}_i^{\text{met}} + \mathbf{F}_i^{\text{rand}} + \zeta_b(\dot{\boldsymbol{\gamma}} \cdot \mathbf{R}_i)$, and H_{ij} is an $N \times N$ symmetric, positive definite, tridiagonal matrix with elements $H_{ii} = 2$ and $H_{ij} = -\mathbf{u}_i \cdot \mathbf{u}_j$ for $i = j \pm 1$.

The metric force $\mathbf{F}_i^{\text{met}}$ for such a free draining chain is given by the derivative

$$\mathbf{F}_i^{\text{met}} = -\frac{1}{2}k_BT\frac{\partial \ln(\det H)}{\partial \mathbf{R}_i} \tag{130}$$

of the "metric pesudopotential" introduced by Fixman (1978) where $\det H$ is the determinant of the matrix with elements H_{ij} introduced above. This metric force must be included in simulations of free-draining chains with constrained rod lengths, in the mid-step algorithm used here, to obtain a Boltzmann distribution $\exp[-U_{\text{bend}}(\mathbf{u}_1, \ldots, \mathbf{u}_N)/k_BT]$ of rod orientations in thermal equilibrium [Fixman (1978), Hinch (1994)]. The metric forces are computed using the algorithm described by Pasquali and Morse (2002).

The stress relaxation function $G(t)$ is obtained from equilibrium simulations, with $\dot{\boldsymbol{\gamma}} = 0$, by using the Kubo relation that relates $G(t)$ to the autocorrelation function of the microscopic stress tensor

$$G(t) = \frac{1}{k_BT}\langle \sigma_{xy}(t)\sigma_{xy}(0)\rangle, \tag{131}$$

where $\boldsymbol{\sigma} \equiv -\Sigma_i\mathbf{R}_i\mathbf{F}_i$ is the contribution of a single chain to the stress tensor. The Brownian contribution to $\boldsymbol{\sigma}(t)$ is calculated using the stochastic filtering method of Grassia and Hinch (1996) and Doyle *et al.* (1997), which avoids including large but temporally uncorrelated contributions to the stress arising from the random force.

To simulate $G(t)$ over a wide range of time scales, we use a technique introduced by Everaers *et al.* (1999) and run simulations with different values of N for each value of L/L_p (where $L = Na$), using simulations with relatively coarse-grained chains (small N) to resolve slow relaxation processes (e.g., rotational diffusion) and shorter simulations of finer-grained chains (large N) to resolve $G(t)$ at shorter times. For each value of N, meaningful results for $G(t)$ are obtained only at times greater than a time proportional to the relaxation time $\zeta a^4/\kappa$ of a bending mode of wavelength a, below which $[G(t)]$ saturates to a finite value whose existence is an artifact arising from the use of a discretized model. The initial chain conformations in each simulation are chosen from an equilibrium Boltzmann distribution. These are generated by an algorithm in which chains are "grown" from one end, by adding each new rod at an orientation chosen randomly from a Boltzmann distribution $e^{-\kappa\mathbf{u}_{i+1}\cdot\mathbf{u}_i/(ak_BT)}$ for the bending energy of the joint between each new rod and the previous one. The use of a pre-equilibrated distribution of initial states allows one to use data from relatively short simulations of fine-grained chains without having to equilibrate the system initially. Results for chains with the same L/L_p but different N are collapsed onto master curves of $[G(t)]$ vs t/τ_{rod}, where $\tau_{\text{rod}} = \zeta_b a^2 N^3/72k_BT$ for the discretized WLC. An example of this collapse is shown in Fig. 6. Ensuing figures show only the regions of overlap of the results obtained with different values of N, which reflect the behavior of a continuous wormlike chain.
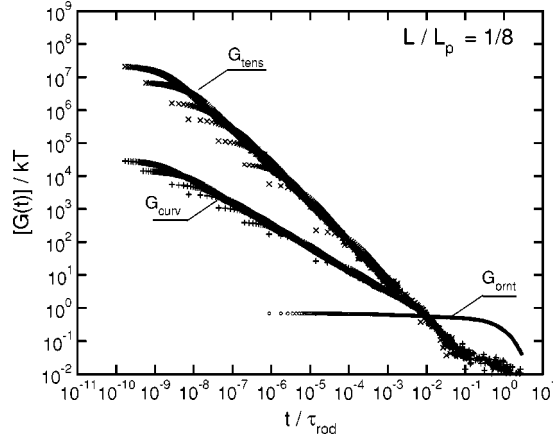
FIG. 6. Simulation results illustrating collapse of simulation data for $[G_{\text{tens}}(t)]$ (top curve, $\times$), $[G_{\text{curv}}(t)]$ (middle curve, $+$), and $[G_{\text{ornt}}(t)]$ (bottom curve, $\bigcirc$) vs t/τ_{rod} with $\tau_{\text{rod}} \equiv \zeta_b N^3 a^2/(72k_B T)$ for $L/L_p = 1/8$ and $N = 8, 16, 22, 32, 46, 64, 90, 128$. $[G_{\text{ornt}}(t)]$ is shown only for the few smallest values of N.

We decompose the stress $\boldsymbol{\sigma}$ obtained from our simulations as a sum $\boldsymbol{\sigma} = \boldsymbol{\sigma}_{\text{ornt}} + \boldsymbol{\sigma}_{\text{curv}} + \boldsymbol{\sigma}_{\text{tens}} - k_B T \mathbf{I}$ of orientational, curvature, and stress components [Morse (1998a)], given by

$$\boldsymbol{\sigma}_{\text{ornt}} \equiv \tfrac{3}{2} k_B T (\mathbf{u}_1 \mathbf{u}_1 + \mathbf{u}_{N-1} \mathbf{u}_{N-1} - 2\mathbf{I}/3), \tag{132}$$

$$\boldsymbol{\sigma}_{\text{curv}} \equiv -\sum_{i=1}^{N} \mathbf{R}_i \mathbf{F}_i^{\text{bend}} + 3k_B T \sum_{i=1}^{N-1} (\mathbf{u}_i \mathbf{u}_i - \mathbf{I}/3) - \boldsymbol{\sigma}_{\text{ornt}}, \tag{133}$$

$$\boldsymbol{\sigma}_{\text{tens}} \equiv \boldsymbol{\sigma} - \boldsymbol{\sigma}_{\text{ornt}} - \boldsymbol{\sigma}_{\text{curv}} + k_B T \mathbf{I}. \tag{134}$$

Corresponding, $[G(t)] = [G_{\text{ornt}}(t)] + [G_{\text{curv}}(t)] + [G_{\text{tens}}(t)]$, where $[G_\alpha(t)]$, with $\alpha = $ "ornt," "curv", or "tens," describes the decay of the stress component $\langle \boldsymbol{\sigma}_\alpha(t) \rangle$ after a small step deformation. These partial intrinsic moduli are calculated from the Kubo relation

$$[G_\alpha(t)] = \frac{1}{k_B T} \langle \sigma_{\alpha,xy}(t) \sigma_{xy}(0) \rangle, \tag{135}$$

which cross correlates components of the single-chain stress with the total.

Figure 7 shows the master curves obtained for the components $[G_{\text{tens}}(t)]$, $[G_{\text{curv}}(t)]$, and $[G_{\text{ornt}}(t)]$ for chains with $L/L_p = 1/8$, $1/4$, $1/2$, and 1, respectively. Also shown, as continuous gray lines, are the predictions of the full theory for these functions. Dashed lines represent the predicted asymptotes for $[G_{\text{tens}}(t)]$ at early and intermediate times [Eqs. (82) and (84)]. Figure 8 shows simulation results and predictions for the total intrinsic modulus $[G(t)]$ (rather than the individual components) for $L/L_p = 1/8$ and $L/L_p = 1$. The theoretical predictions were obtained by numerically Fourier transforming the results of the full theory for the tension and curvature components to $[G^*(\omega)]$, using isotropic friction coefficients, $\zeta_\parallel = \zeta_\perp = \zeta_b/a$, as in the simulations.

Consider first the stiffest chains simulated, with $L/L_p = 1/8$. For these, we obtain excellent agreement between theory and simulations over the entire range of time scales
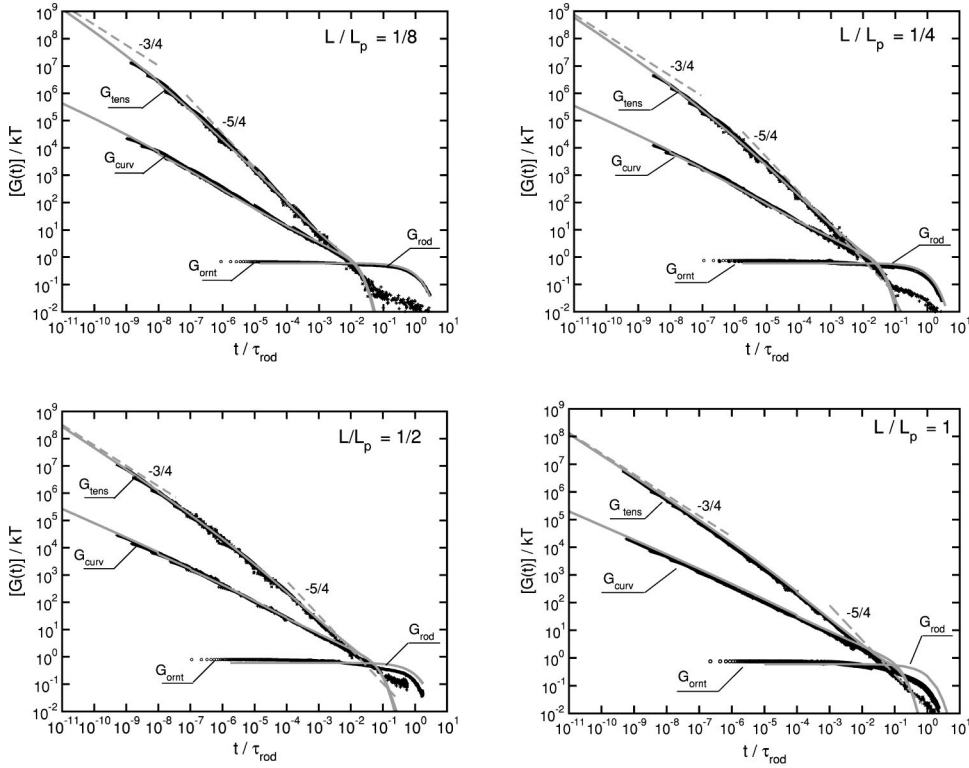
FIG. 7. Comparison of theory and simulations for different values of L/L_p: Data points (black symbols) represent simulation results for $[G_{tens}(t)]$ (top curve, $\times$), $[G_{curv}(t)]$ (middle curve, $+$), and $[G_{ornt}(t)]$ (bottom curve, $\bigcirc$), plotted vs t/τ_{rod} with $\tau_{rod} \equiv \zeta_b N^3 a^2/(72 k_B T)$. Continuous gray lines are our theoretical results for these three components $G(t)$. Short dashed gray lines are predicted asymptotic power laws as indicated.

accessible to simulations. This set of simulations clearly show a broad intermediate regime where $[G_{tens}(t)] \sim t^{-5/4}$, but does not access the $t^{-3/4}$ decay predicted at extremely early times, which was computationally inaccessible. A clear orientational plateau, with $[G(t)] \simeq [G_{ornt}(t)] \simeq \frac{3}{5} k_B T e^{-t/\tau_{rod}}$, is also visible at times approaching
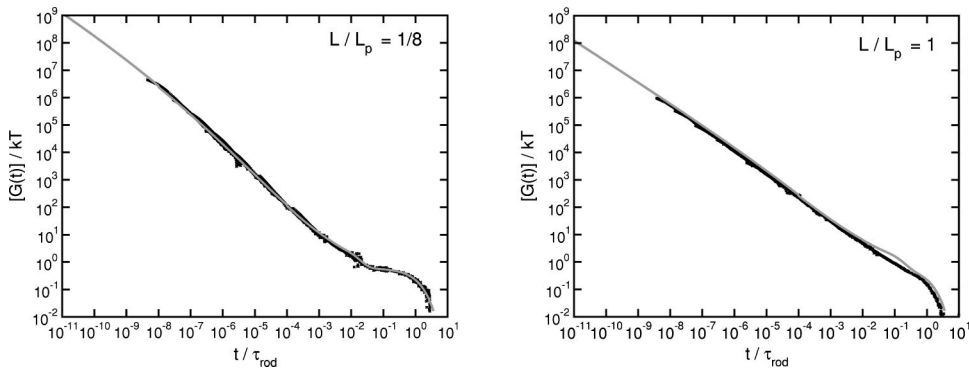

FIG. 8. Comparison between theoretical prediction (gray lines) and the results of Brownian dynamics simulations (black symbols) for the intrinsic modulus $[G(t)]$ vs t/τ_{rod}, for $L/L_p = 1/8$ (left panel) and $L/L_p = 1$ (right panel).

τ_{rod}. As L/L_p is increased from 1/8 to 1/4, 1/2, and 1 in the remaining simulations, the intermediate regime gradually disappears, as $\tau_{\parallel}$ (rapidly) and $\tau_{\perp}$ (more slowly) approach τ_{rod}, while the predicted $t^{-3/4}$ regime moves into the computationally accesible window. For the most flexible chains shown, with $L/L_p = 1$, both the intermediate regime and the orientational plateau are absent, but the simulation results begin to closely approach the early time $t^{-3/4}$ asymptote. The predictions of the full theory become noticeably less accurate with increasing L/L_p, as expected for a theory that is based upon an expansion about a rigid rod reference, but remain remarkably accurate for chains of length up to $L = L_p$. For the most flexible chains, with $L = L_p$, the predictions of the individual components of $[G(t)]$ are noticeably less accurate at times approaching τ_{rod} than the predictions of the total $[G(t)]$, indicating a partial compensation of errors.

Simulations very similar to those discussed above and in our earlier report [Pasquali *et al.* (2001)] have also been carried out by Dimitrakopoulos *et al.* (2001). These authors reported that their simulation results for $[G(t)]$ could be adequately fit over a wide range of intermediate times by a single power-law decay $[G(t)] \propto t^{-\alpha}$, with an apparent exponent α that varies continuously with L/L_p and approaches $\alpha = 5/4$ for $L/L_p \ll 1$. This description is broadly consistent with the simulation data of both groups: For example, the simulation data for $[G(t)]$ for $L/L_p = 1$ in Fig. 8 is fit well by a $t^{-7/8}$ power law, as reported by these authors. The theory shows, however, that this is an empirical description of a broad crossover in both time and L/L_p, which can be accurate only at intermediate values of L/L_p, since universal power laws are predicted for $L \ll L_p$ and $L \gg L_p$, and only in an intermediate range of computationally accessible times, since a universal $t^{-3/4}$ decay is expected at early times for all L/L_p.

X. COMPARISON WITH EXPERIMENTS

In this section, we compare our predictions with the experimental data of Warren *et al.* (1973) and Ookubo *et al.* (1976), who carried out linear viscoelastic measurements of $G'(\omega)$ and $G''(\omega)$ for dilute solutions of PBLG in the solvent *m*-Cresol. The persistence length of PBLG is approxiamtely 150 nm, though there does not appear to be a consensus in the literature on the exact value; reported estimates range from 100 to 180 nm. The average lengths of the chains used in the experiments of Warren *et al.* (1973) include $L = 108$ and 162 nm, while Ookubo *et al.* (1976) used chains with $L = 116$, 82, and 51 nm. The chain lengths in most of these experiments are thus comparable to the persistence length. Although our theory is constructed so as to be accurate only in the limit $L/L_p \ll 1$, a comparison between the theory and these experiments seems reasonable in light of the level of agreement found above between the theory and Brownian dynamics simulations of chains with comparable values of L/L_p.

A. Experiments of Warren *et al.*

Warren *et al.* (1973) used a multiple-lumped resonator to measure $[G^*(\omega)]$ of dilute solutions of PBLG in *m*-Cresol with molecular weights ranging from 16×10^4 to 57×10^4 in the frequency range 106–6060 Hz and concentration range 0.0015–0.005 g/ml. They reported intrinsic moduli data, which were obtained by extrapolation to infinite dilution, for three samples containing chains of length 108, 162, and 387 nm. We compare the theory only to data from the samples with $L = 108$ and 162 nm, since L significantly exceeds L_p for the third sample. Warren *et al.* (1973) report a polydispersity index $M_w/M_n = 1.234$ for these samples.

We take into account polydispersity in the theory by calculating an average
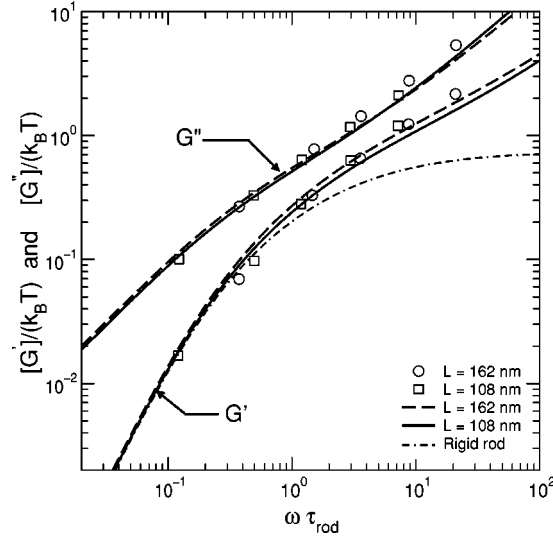
FIG. 9. Comparison with the experiments of Warren *et al.* (1973): Intrinsic storage modulus $[G']/(k_BT)$ and loss modulus $[G'']/(k_BT)$ as a function of reduced frequency $\omega\tau_{\text{rod}}$ for two different (average) lengths $L = 108$ nm, $L = 162$ nm. τ_{rod} for the experiments is determined from $\pi\eta_s L^3/[18k_BT\ln(L/d)]$ where $d = 2.5$ nm. Symbols $\bigcirc$ ($L = 162$ nm) and $\square$ ($L = 108$ nm) are the data from Warren *et al.* (1973) and the lines are theoretical predictions for $L_p = 130$ nm. Also shown as a dash-dotted line is the predicted $[G'(\omega)]$ for true rigid rods.

$$G(t) = \int_0^\infty dL\ \nu(L)[G(t;L)], \tag{136}$$

where $[G(t;L)]$ is the predicted intrinsic modulus for chains with length L, and $\nu(L)dL$ is the number of chains per unit volume with contour length between L and $L+dL$. We assume a distribution of the form

$$\nu(L) \propto \left(\frac{L}{L_0}\right)^\alpha \exp[-L/L_0], \tag{137}$$

where L_0 is chosen to obtain a weight averaged length equal to the reported value. We use an exponent $\alpha = 3$, which yields a polydispersity index of 1.25 very close to the reported value.

In Fig. 9, we compare theoretical predictions and the data reported by Warren *et al.* (1973) (digitized from their Fig. 4) for the ratio $[G^*(\omega)]/(k_BT)$ vs $\omega\tau_{\text{rod}}$. We have followed Warren *et al.* in plotting data for chains with two different lengths ($L = 108$ nm and $L = 162$ nm) in a single graph, as in their Fig. 4, because the resulting data very nearly superpose for these two samples. Theoretical predictions for both reported chain lengths are calculated using a persistence length $L_p = 130$ nm, with anisotropic friction coefficients $\zeta_\perp = 2\zeta_\parallel$. Frequencies in the theoretical curves have been rescaled using $\tau_{\text{rod}} = \zeta_\perp L^3/(72k_BT)$, where L is the length averaged chain length. The experimental data in this and all other plots have been made dimensionless using the rotational diffusion time $\tau_{\text{rod}} = \pi\eta_s L^3/[18k_BT\ln(L/d)]$ predicted by slender-body hydrodynamics, where L is the reported weight-averaged chain length, using the hydrodynamic chain diameter of $d = 2.5$ nm reported by Warren *et al.* (1973) and the reported solvent viscosity. Also shown in this figure is the storage modulus predicted by the rigid rod theory
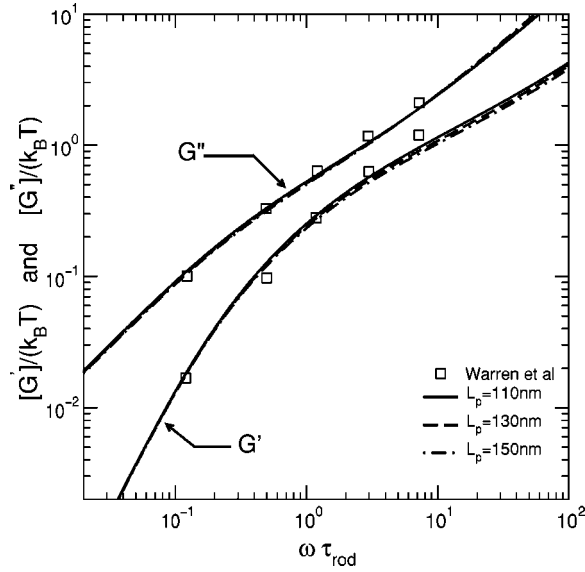
FIG. 10. Effect of variations of L_p on the theoretical prediction (lines), and on the comparison with the data ($\square$) of Warren *et al.* (1973): $[G']/(k_BT)$ and $[G'']/(k_BT)$ vs $\omega\tau_{\text{rod}}$ for $L = 108$ nm, for $L_p = 110$, 130, and 150 nm.

(corrected for polydispersity) which agrees well with the data in the terminal regime but clearly fails at higher frequencies. Like the experimental data, our predictions for the two different chain lengths are only slightly different, despite the 50% difference in L, indicating that both the predicted and measured shape of the curves in this representation change only slowly with changes in the ratio L/L_p for $L \simeq L_p$. The same point is evident in Fig. 10, where we show the effect of varying L_p from 110 to 150 nm on the theoretical predictions for $L = 108$ nm. Aside from the uncertainty introduced by the existence of a substantial range of estimated values for the persistence length of PBLG in the literature, which seems to have a weak effect on our predictions, this comparison with experiment contains no adjustable parameters.

B. Experiments of Ookubo *et al.*

Ookubo *et al.* (1976) used a torsional free decay method to measure linear viscoelastic measurements of dilute PBLG solutions in *m*-Cresol at concentrations 0.002–0.05 gm/ml in a frequency range $2.2\times10^3 - 5.25\times10^5$ Hz, giving a maximum frequency an order of magnitude larger than that obtained by Warren *et al.* (1973). These authors, who reported measurements of the complex viscosity $\eta^*(\omega) \equiv \eta'(\omega) - i\eta''(\omega) = G^*(\omega)/(i\omega)$, reported that their accuracy for $\eta'(\omega) = G''(\omega)/\omega$ is higher than that for $\eta''(\omega) = G'(\omega)/\omega$, and that the lack of accuracy of their data for $\eta''(\omega)$ made extrapolation to infinite dilution to impossible for this component. We thus consider the data of Ookubo *et al.* (1976) to be less reliable than that of Warren *et al.* (1973). We nevertheless have compared the theory with this data because it contains data for both shorter chain lengths and significantly higher frequencies than those reported by Warren *et al.* (1973).

Ookubo *et al.* (1976) carried out measurements on three fractionated samples, with lengths $L = 116$, 82, and 51 nm, and one unfractionated sample, which we do not consider. No value for the polydispersity index is reported, and so, in the absence of a better estimate, we assume a polydispersity of 1.25 similar to that reported by Warren *et al.*
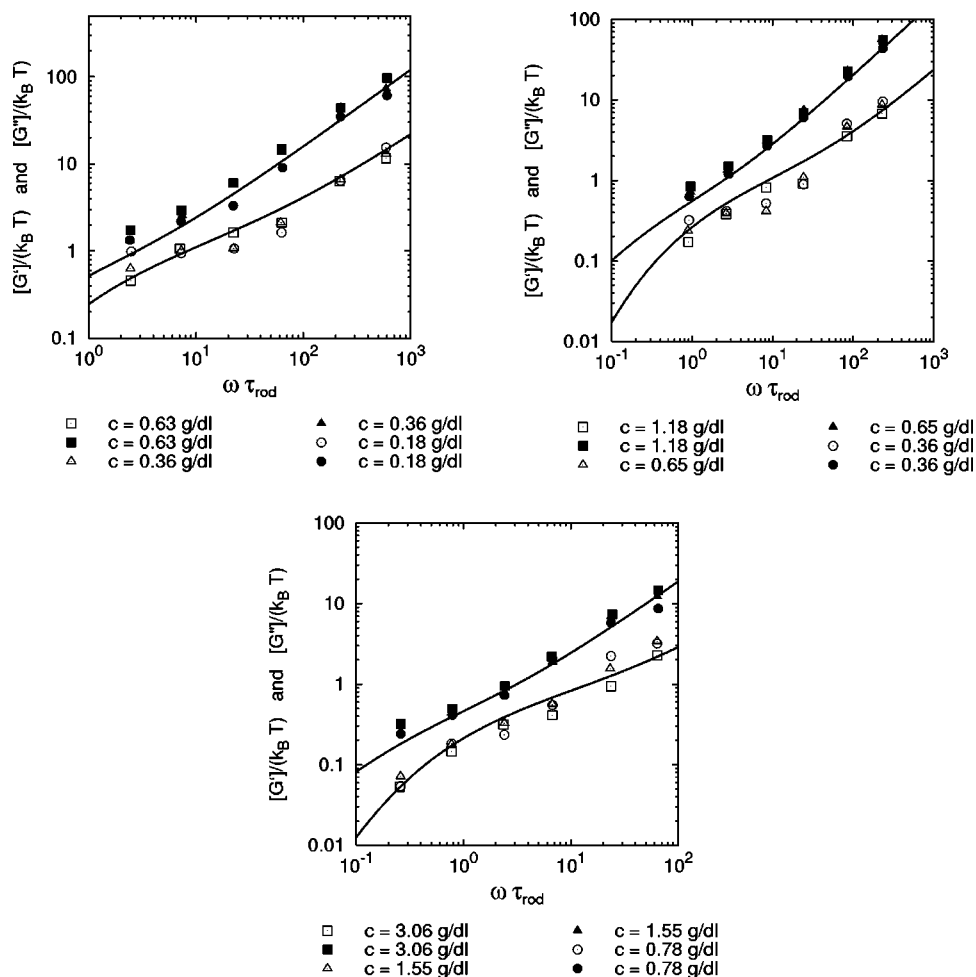
FIG. 11. Comparison with the experiments of Ookubo *et al.* (1976) for different values of *L*: Intrinsic storage modulus $[G']/(k_BT)$ and loss modulus $[G'']/(k_BT)$ as a function of $\omega\tau_{rod}$ for three different chain lengths indicated above, with at several concentrations per chain length. Symbols are the data from Ookubo *et al.* (1976) and the lines are from our theory with $L_p = 130$ nm. Unfilled symbols represent storage modulus and filled symbols represent loss modulus.

Figures 11(a)–11(c) show the values of $[G']/(k_BT)$ and $[G'']/(k_BT)$ vs $\omega\tau_{rod}$ obtained for these three chain lengths at all of the reported concentration. The intrinsic moduli in these graphs are calculated from the digitized plots of Ookubo *et al.* (1976) for $\eta''(\omega)$ and $\eta'(\omega)$ by dividing the resulting $G'(\omega)$ and $G''(\omega) - i\omega\eta_s$ by the actual concentration, rather than by extrapolating to infinite dilution. Values of τ_{rod} are calculated, as before, using reported chain lengths and solvent viscosity of $\eta_s = 0.105$ P. The solid lines are corresponding theoretical predictions for the intrinsic moduli, calculated for $L_p = 130$ nm, for these three chain lengths. The lack of a smooth variation of the data for $[G'(\omega)]$ with concentration explains the authors' conclusion that this data cannot support a meaningful extrapolation to infinite dilution. Figures 11(a)–11(c) indicate that there is nonetheless good agreement between theoretical and experimental results for
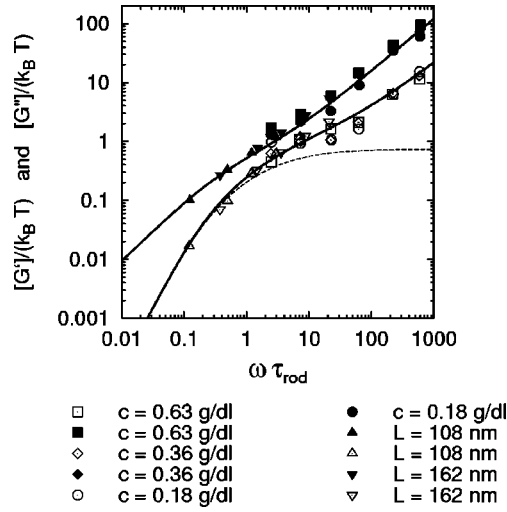
FIG. 12. Attempted data collapse of intrinsic storage and loss modulus data reported in Warren *et al.* (1973) ($L = 108$, 162 nm) and Ookubo *et al.* (1976) ($L = 116$ nm) as a function of $\omega\tau_{\rm rod}$. Symbols denote the data at different concentrations of Ookubo *et al.* (1976) and the two different lengths of Warren *et al.* (1973). All unfilled symbols represent storage modulus data and filled symbols represent loss modulus data. Solid lines are our theoretical predictions for $L = 116$ nm and $L_p = 130$ nm. The dotted line is the predicted $[G'(\omega)]/(k_B T)$ for rigid rods.

$[G''(\omega)]$ and (in light of the evident experimental uncertainties) reasonable agreement for $[G'(\omega)]$ at all three chain lengths.

In Fig. 12, we have combined the infinite dilution data of Warren *et al.* (1973) with $L = 108$ and 162 nm, which have already been shown to nearly superpose, together with the data of Ookubo *et al.* at several concentrations for the fraction with $L = 116$ nm. In general, there is good collapse of these three data sets, over a combined frequency range of nearly four decades, which is substantially wider than that obtained in any single measurement. Theoretical predictions for $L = 116$ nm and $L_p = 130$ nm agree well with this data over this entire range.

XI. AN ANALYTIC APPROXIMATION

The LCA results for the stress relaxation modulus $G(t)$ and related quantities such as the single chain compliance $\chi(t)$ agree well with the results of the full theory at short times, less than the longest transverse relaxation time $\tau_\perp / \alpha_1^4$, but fail at longer times because the approximation uses a continuous distribution of Fourier modes rather than discrete set of bending modes, and thus contains no terminal relaxation time. As a result, the LCA predicts power law decays for the tension and curvature contribution to $G(t)$ even at times $t \gg \tau_\perp$, whereas the full theory predicts exponential decay of these components with relaxation times proportional to $\tau_\perp / \alpha_1^4$.

A physically motivated approximation to the full theory can thus be obtained by taking the LCA results for these components of $G(t)$ and multiplying them by an exponential cutoff, i.e., by approximating

$$G_\alpha(t) \simeq G_{\alpha,\rm LCA}(t) e^{-t/\tau_\alpha}, \tag{138}$$

where $G_{\alpha,\text{LCA}}(t)$ is the LCA prediction for component α of $G(t)$, and τ_α is a time proportional to $\tau_\perp$. Corresponding analytic approximations for the components of $G^*(\omega)$ can be obtained by using the following property of Fourier transforms: If

$$G(t) = F(t)e^{-t/\tau}, \tag{139}$$

then the one-sided Fourier transform $\tilde{G}(\omega) \equiv \int_0^\infty dt\, G(t) e^{-i\omega t}$ of $G(t)$ is given by

$$\tilde{G}(\omega) = \int_0^\infty dt\, F(t)e^{-t/\tau}e^{-i\omega t} = \tilde{F}(\omega - i\tau^{-1}), \tag{140}$$

i.e., by the analytic continuation of the one-sided transform $\tilde{F}(\omega)$ of $F(t)$ to a complex frequency $\omega - i\tau^{-1}$. The one-sided Fourier transform of $G(t)$ is given by the ratio $\tilde{G}(\omega) \equiv G^*(\omega)/(i\omega) = \int_0^\infty dt\, G(t)e^{-i\omega t}$, so this prescription requires us to analytically continue the LCA predictions for components of $G^*(\omega)/(i\omega)$, rather than of $G^*(\omega)$.

We obtain analytic approximations for the tension and curvature components of $G^*(\omega)$ by evaluating the analytic LCA predictions for the components $G^*_{\text{tens}}(\omega)/i\omega$ and $G^*_{\text{curv,t}}(\omega)/i\omega$, and for the ratio $G^*_{\text{curv,l}}(\omega)/G^*_{\text{tens}}(\omega)$, at complex frequencies with imaginary parts proportional to $-\alpha_1^4\tau_\perp^{-1}$. This yields

$$[G^*_{\text{tens}}(\omega)] \simeq \frac{1}{15}LB(\omega)\left[1 - \frac{\tanh[\lambda(\omega_1)/2]}{\lambda(\omega_1)/2}\right]\frac{\omega}{\omega_1},$$

$$[G^*_{\text{curv,l}}(\omega)] \simeq \frac{3}{2^{5/4}}\frac{L}{L_p}(i\omega_2\tau_\perp)^{-1/4}[G^*_{\text{tens}}(\omega)], \tag{141}$$

$$[G^*_{\text{curv,t}}(\omega)] \simeq \frac{3}{2^{3/4}10}(i\omega_3\tau_\perp)^{1/4}\frac{\omega}{\omega_3},$$

where $\lambda(\omega_1) \equiv [i\omega_1\zeta_\parallel L^2/B(\omega_1)]^{1/2}$ is calculated by evaluating Eq. (7) for $B(\omega)$ at a complex frequency ω_1, and in which ω_1, ω_2, and ω_3 are three complex frequencies, of the form

$$\omega_i \equiv \omega - iC_i\alpha_0^4\tau_\perp^{-1} \tag{142}$$

with $i = 1,.2,3$ with different numerical constants C_1, C_2, and C_3. These numerical constants are treated as fitting parameters, which are adjusted to optimize the fit of the resulting approximation to the results of the full theory. The choice $C_1 = 0.14$, $C_2 = 0.72$, and $C_3 = 1.26$ yields an approximation of the total loss and storage moduli that differs from the results of full theory by less than 6% at any frequency for $L/L_p = 1/8$, 1/4, 1/2, and 1. The approximate storage and loss moduli obtained for $L/L_p = 1/8$ with these constants are compared with the results of the full theory in Fig. 5.

XII. RELATION TO THE HARRIS AND HEARST MODEL

We now compare our theoretical predictions for linear viscoelastic moduli to those of Harris and Hearst (1966) and Hearst *et al.* (1966) (HH), who also attempted to calculate linear viscoelastic moduli for dilute solutions of wormlike chains. These authors considered a generalized Gaussian approximation for a wormlike chain, in which the equilibrium distribution of contour $\mathbf{R}(s)$ is controlled by an effective potential energy

$$U = \frac{1}{2}\int_0^L ds \left[\kappa \left(\frac{\partial^2 \mathbf{R}}{\partial s^2} \right)^2 + \mathcal{T} \left(\frac{\partial \mathbf{R}}{\partial s} \right)^2 \right], \tag{143}$$

in which $\mathcal{T}$ is a Lagrange multiplier introduced to impose approximately the constraint of constant length. In this model, however, $\mathcal{T}$ is not treated as a fluctuating field, but as a constant, which is independent of both s and t. The value of $\mathcal{T}$ for a given chain length L is chosen to yield an equilibrium mean-squared end-to-end distance equal to that of a true wormlike chain of equal length. Harris and Hearst (1966) find that, in the rodlike limit $L \gg L_p$ of interest here, this criterion yields a value $\mathcal{T} \simeq 3k_BT/L$. While the HH model can be applied to chains of arbitrary length, we consider only its predictions for the rodlike limit, $L \ll L_p$.

The dynamical equation used by Harris and Hearst (1966) is identical to our Eq. (2), except for the crucial fact that HH treat the tension $\mathcal{T}$ as a constant, independent of s, t, and the state of flow. Their model thus does not allow any tension to be induced in the chain by flow. HH expand all three Cartesian components of the chain contour $\mathbf{R}(s)$ in eigenfunctions of the eigenvalue problem

$$\frac{\partial^4 \mathcal{W}_j}{\partial \hat{s}^4} - \Lambda \frac{\partial^2 \mathcal{W}_j}{\partial \hat{s}^2} = \alpha_j^4 \mathcal{W}_j, \tag{144}$$

with $\Lambda \equiv \mathcal{T}L^2/\kappa$, with corresponding boundary conditions

$$\frac{\partial^2 \mathcal{W}_j}{\partial \hat{s}^2} = 0, \qquad \frac{\partial^3 \mathcal{W}_j}{\partial \hat{s}^3} - \Lambda \frac{\partial \mathcal{W}_j}{\partial \hat{s}} = 0 \tag{145}$$

at both chain ends. Equations (144) and (145) reduce to our Eqs. (101) and (102) in the limit $\Lambda \to 0$. In the rodlike limit, $L \ll L_p$, where the coefficient $\Lambda \simeq 3L/L_p$ is small, the presence of the second derivative term in Eq. (144) has a significant effect only on the smallest eigenvalue α_0, which vanishes when $\Lambda = 0$. We find by a perturbation analysis of Eqs. (144) and (145) that the presence of a small nonzero $\Lambda = 3L/L_p$ splits the degeneracy between the two zero modes of our Eq. (100), yielding a vanishing eigenvalue for the translation mode, with $\mathcal{W} \propto$ const., but producing a small nonzero eigenvalue $\alpha_0^4 \simeq 36L/L_p$ for the eigenvector $\mathcal{W} \propto (\hat{s} - 1/2)$ that, in Eq. (100), represents rigid rotations.

In the present notation, the Harris and Hearst (1966) result [their Eq. (55)] for the complex modulus is

$$[G_{HH}^*(\omega)] = k_BT \sum_{i=0}^{\infty} \frac{i\omega}{i\omega + 2\tau_\perp^{-1}\alpha_i^4}. \tag{146}$$

In the rodlike limit, the eigenvalues α_i can be approximated by those obtained with $\Lambda = 0$, except for the $i = 0$ mode, for which $\alpha_0^4 = 36L/L_p$. Comparing the relaxation rate $2\tau_\perp^{-1}\alpha_0^4$ of the contribution arising from the $i = 0$ mode to the relaxation rate τ_{rod}^{-1} for the orientational stress in a solution of rods shows that they are equal

$$\tau_{rod}^{-1} = 2\tau_\perp^{-1}\alpha_0^4 = \frac{72k_BT}{\zeta_\perp L^3}. \tag{147}$$

Separating the contribution of the $i = 0$ mode from the remaining sum in Eq. (146) yields

$$\lim_{L \ll L_p} [G_{HH}^*(\omega)] = k_B T \frac{i\omega}{i\omega + \tau_{rod}^{-1}} + k_B T \sum_{i=1}^{\infty} \frac{i\omega}{i\omega + 2\tau_\perp^{-1}\alpha_i^4}. \tag{148}$$

The first term on the rhs of Eq. (148) resembles Eq. (93) for $[G_{ornt}^*(\omega)]$, and the remaining sum over $i \geqslant 1$ resembles Eq. (121) for $[G_{curv,t}^*(\omega)]$. However, our Eqs. (93) and (121) each contain a prefactor of 3/5 that is absent from either term on the rhs of Eq. (148); thus, the HH result for $[G^*(\omega)]$ in the rodlike limit is related to our results by

$$\tfrac{3}{5}[G_{HH}^*(\omega)] = [G_{ornt}^*] + [G_{curv,t}^*], \tag{149}$$

where the two terms on the rhs are given by Eqs. (93) and (121), respectively.

This relationship shows that, in the rodlike limit, the Harris–Hearst model neglects the two contributions to $[G^*(\omega)]$ that dominate at intermediate and high frequencies, viz. $[G_{tens}^*]$ and $[G_{curv,l}^*]$, which both arise from flow induced tension, while retaining contributions that (aside from a different prefactor) resemble $[G_{curv,t}^*]$ and $[G_{ornt}^*]$, which are subdominant at these frequencies. As a result, the HH model predicts storage and loss moduli that increase as $\omega^{1/4}$ at $\omega \gg \tau_\perp^{-1}$, like our $[G_{curv,t}^*(\omega)]$, and so enormously underestimates $[G'(\omega)]$ at all $\omega \gg \tau_\perp^{-1}$ and $[G''(\omega)]$ at all $\omega \gg \tau_{rod}^{-1}$, as shown in Fig. 13. The model's predictions are less egregiously wrong at lower frequencies: At $\omega \ll \tau_\perp^{-1}$, where $[G'(\omega)]$ is dominated by the orientational stress, the model correctly predicts a Maxwellian behavior for $[G'(\omega)]$, with the correct relaxation rate τ_{rod}^{-1}, but with a numerical prefactor that is too large by 5/3. Interestingly, the model predicts the correct intrinsic zero shear viscosity of $[\eta_0] = k_B T \tau_{rod}$ for a model of rods with isotropic friction, because the use of too large a prefactor for the "orientational" contribution to η_0 (i.e., the $i = 0$ mode) is exactly compensated by the absence of a tension contribution. This success is a consequence of the fact that the zero shear viscosity of such a free-draining model depends only on the polymer's equilibrium radius of gyration R_g [see Eq. (16.3-20) of Bird *et al.* (1987)], and that the model gives the correct limiting value for R_g in the rodlike limit.

XIII. CONCLUDING REMARKS

This paper presents a theory that describes accurately the linear viscoelastic response of dilute solutions of freely draining semiflexible rods, with lengths L smaller than their persistence lengths L_p, over the whole range of possible frequency and time scales. The theory treats the inextensible wormlike chain as an effectively extensible rod with an effective longitudinal compliance that arises from the existence of transverse thermal fluctuations. A simplified, analytically solvable local compliance approximation, which ignores the spatial nonlocality of the relationship between the average tension and strain fields, describes accurately the viscoelastic behavior throughout the intermediate and high frequency regimes in which the predicted behavior differs significantly from that of rigid rods.

In the limit of very stiff chains, the theory predicts a stress relaxation modulus $G(t)$ that decays as $t^{-3/4}$ at very early times, as found previously by Morse (1998b) and Gittes and MacKintosh (1998), but that decays as $t^{-5/4}$ over a range of intermediate times $\tau_\parallel < t < \tau_\perp$, which broadens rapidly as L/L_p decreases. At times larger than the relaxation time $\tau_\perp$ of the longest bending mode, the theory predicts an exponential decay $G(t) \propto e^{-t/\tau_{rod}}$ identical to that found for rigid rods. This description is accurate, however, only for very stiff rods: As L approaches L_p from below, the times $\tau_\parallel, \tau_\perp$, and τ_{rod}
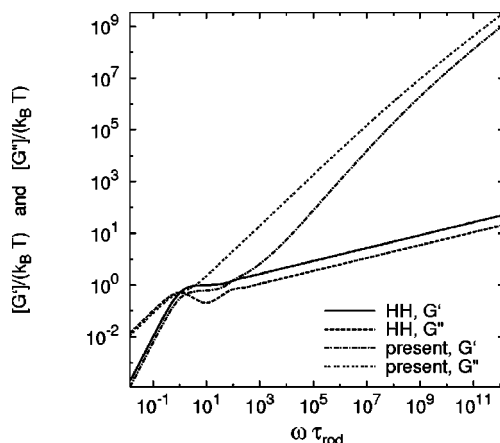
FIG. 13. Comparison of the present theoretical predictions with the theoretical results of Harris and Hearst (1966) (denoted as HH in the figure): Intrinsic storage and loss moduli vs $\omega \tau_{\text{rod}}$ for $L/L_p = 1/8$.

approach one another, and hence both the intermediate $t^{-5/4}$ decay and the rigid rod orientational plateau disappear gradually. An initial $t^{-3/4}$ decay of $G(t)$ is expected for any value of L/L_p, but only below a time $\tau_\parallel \propto \tau_{\text{rod}}(L/L_p)^5$ that remains much lower than τ_{rod} even for $L \sim L_p$ and that drops with decreasing L/L_p to values that, for $L \ll L_p$, rapidly become inaccessible to either our simulations or experiment. The intermediate time $t^{-5/4}$ decay in $G(t)$, and the corresponding intermediate $\omega^{5/4}$ frequency dependence of $G'(\omega)$, is observable at more easily accessible times and frequencies, but is well defined only for very stiff chains. In light of the resulting difficulties facing any attempt compare our asymptotic power law predictions directly to experiment, we wish to emphasize that the full theory and the analytic approximation of Sec. XI both provide accurate predictions over much wider ranges of frequency and reduced chain length L/L_p than those provided by asymptotic analysis alone.

In the opposite limit of a dilute solutions of coillike chains, with lengths much larger than a few persistence lengths, we expect a $t^{-3/4}$ decay at very early times followed by a Rouse-like $t^{-1/2}$ decay at longer times for models of free-draining chains, or a Zimm-like decay for very long chains with hydrodynamic interactions. Thus, with the results of the present study, theoretical understanding of the linear viscoelasticity of dilute solutions of freely draining wormlike chains is nearly complete for the whole range of L/L_p from rigid rods ($L/L_p \to 0$) to random coils ($L/L_p \gg 1$), except for a small (in a logarithmic sense) crossover region in which L is somewhat larger than L_p, where there must be a crossover from the behavior described here to a Rouse–Zimm behavior.

Comparison of the theoretical predictions to the results of our Brownian dynamics simulations of stress relaxation show striking quantitative agreement over roughly nine orders of magnitude in time. Predictions of $G(t)$ remain reasonably accurate for chains of length up to $L = L_p$, despite the expansion about a rigid-rod reference state that is used throughout the derivation of the theory. We have also compared the theory with the available linear viscoelastic data for dilute solutions of rodlike poly (γ-benzyl-L-glutamate) in m-Cresol [Warren *et al.* (1973), Ookubo *et al.* (1976)]. These data are for chains with $L/L_p \simeq 0.4$–1.2 at reduced frequencies of $\omega \tau_{\text{rod}} \simeq 10^{-1}$–$10^4$, which is a crossover region in which none of the asymptotic power laws are valid. The predictions of the full theory are nonetheless found to be in good quantitative agreement with these experiments, with essentially no adjustable parameters.

ACKNOWLEDGMENTS

APPENDIX

In this appendix, we calculate the response function $\Theta(s,\omega)$ defined in Eq. (28), which describes the direct response of $\langle \mathcal{E}(s,\omega) \rangle$ to the velocity gradient that appears in transverse dynamical Eq. (24). Here, as in the full theory of Sec. VIII, we use eigenvector expansion (100) for $h_\alpha(s)$, expansion (105) of the transverse dynamical equation, and expansion (107) of the average strain field. A calculation similar to that used to obtain Eq. (120) shows that the velocity gradient term in Eq. (105) introduces a contribution to $a_{kl}(\omega)$ given by

$$a_{kl}(\omega) = \delta_{kl} \frac{k_B T L^3}{\kappa \alpha_k^4} \frac{i\omega \zeta_\perp}{i\omega \zeta_\perp + 2\alpha_k^4 \tau_\perp^{-1}} \sum_\alpha \gamma_{\alpha\alpha}(\omega). \tag{A1}$$

Substituting this into Eq. (107), and using the expression $\Sigma_\alpha \gamma_{\alpha\alpha}(\omega) = \boldsymbol{\gamma}(\omega){:}(\mathbf{I}-\mathbf{nn})$ $= -\boldsymbol{\gamma}(\omega){:}\mathbf{nn}$ for traceless $\boldsymbol{\gamma}(\omega)$ yields a strain of the form $\langle \mathcal{E}(s,\omega) \rangle$ $= \Theta(s,\omega) \boldsymbol{\gamma}(\omega){:}\mathbf{nn}$, where

$$\Theta(s,\omega) = \frac{L}{L_p} \sum_k \left(\frac{\partial \mathcal{W}_k}{\partial \hat{s}} \right)^2 \frac{1}{\alpha_k^4 [1 + 2\alpha_k^4 (i\omega\tau_\perp)^{-1}]}. \tag{A2}$$

The rhs of Eq. (A2) is a factor of L/L_p times a dimensionless function of $\hat{s}$ and $\omega\tau_\perp$ alone, which is defined by the sum. This sum increases linearly with $i\omega\tau_\perp$ for $\omega\tau_\perp \ll 1$, and approaches a finite limit for $\omega \gg \tau_\perp^{-1}$. In the rodlike limit $L/L_p \ll 1, \Theta(s,\omega)$ is thus always small compared to unity as a result of the overall prefactor of L/L_p. This justifies our neglect of this contribution in the main text, as discussed in Sec. III.

References

Aragon, S. R. and R. Pecora, "Dynamics of wormlike chains," Macromolecules **18**, 1868–1875 (1985).

Batchelor, G. K., "Slender-body theory for particles of arbitrary cross-section in stokes flow," J. Fluid Mech. **44**, 419–420 (1970).

Bird, R. B., C. F. Curtiss, R. S. Armstrong, and O. Hassager, *Dynamics of Polymeric Liquids, Vol. 2: Kinetic Theory* (Wiley, New York 1987).

Carriere, G. J., E. Amis, J. L. Schrag, and J. D. Ferry, "Dilute solution dynamic viscoelastic properties of schizophyllan polysaccharide," Macromolecules **18**, 2019–2023 (1985).

Carriere, G. J., E. Amis, J. L. Schrag, and J. D. Ferry, "Dilute solution dynamic viscoelastic properties of xanthan polysaccharide," J. Rheol. **37**, 469–478 (1993).

Dimitrakopoulos, P., J. F. Brady, and Z.-G. Wang, "Short- and intermediate-time behavior of the linear stress relaxation in semiflexible polymers," Phys. Rev. E **64**, 050803(R) (2001).

Doi, M. and S. Edwards, *The Theory of Polymer Dynamics* (Clarendon, Oxford, 1986).

Doyle, P. S., E. S. G. Shaqfeh, and A. P. Gast, "Dynamic simulation of freely draining flexible polymers in steady linear flows," J. Fluid Mech. **334**, 251–291 (1997).

Everaers, R, F. Julicher, A. Ajdari, and A. C. Maggs, "Dynamic fluctuations of semiflexible filaments," Phys. Rev. Lett. **82**, 3717–3720 (1999).

Fixman, M., "Simulation of polymer dynamics. I. General theory," J. Chem. Phys. **69**, 1527–1537 (1978).

Gittes, F. and F. C. MacKintosh, "Dynamic shear modulus of a semiflexible polymer network," Phys. Rev. E **58**, R1241–R1243 (1998).

Granek, R., "From semiflexible polymers to membranes: Anomalous diffusion and reptation," J. Phys. II **7**, 1761–1788 (1997).

Grassia, P. S. and E. J. Hinch, "Computer simulation of polymer chain relaxation of Brownian motion," J. Fluid Mech. **308**, 255–288 (1996).

Harris, R. A. and J. E. Hearst, "On polymer dynamics," J. Chem. Phys. **44**, 2595–2602 (1966).

Hearst, J., R. A. Harris, and E. Beals, "On polymer dynamics. II," J. Chem. Phys. **45**, 3106–3133 (1966).

Hinch, E. J., "The distortion of a flexible inextensible thread in a shearing flow," J. Fluid Mech. **74**, 317–333 (1976).

Hinch, E. J., "Brownian motion with stiff bonds and rigid constraints," J. Fluid Mech. **271**, 219–234 (1994).

Kirkwood, J. and P. Auer, "Viscoelasticity of solutions of rodlike macromolecules," J. Chem. Phys. **19**, 281–283 (1951).

Kroy, K. and E. Frey, "Dynamic scattering from solutions of semiflexible polymers," Phys. Rev. E **55**, 3092–3101 (1997).

Liverpool, T. B. and A. C. Maggs, "Dynamic scattering from semiflexible polymers," Macromolecules **34**, 6064–6073 (2001).

MacKintosh, F. C., J. Kas, and P. A. Janmey, "Dynamic shear modulus of a semiflexible polymer network," Phys. Rev. Lett. **58**, 4425–4428 (1995).

Morse, D. C., "Viscoelasticity of concentrated isotropic solutions of semiflexible polymers. 1. Model and stress tensor," Macromolecules **31**, 7030–7043 (1998a).

Morse, D. C., "Viscoelasticity of concentrated isotropic solutions of semiflexible polymers. 2. Linear response," Macromolecules **31**, 7044–7067 (1998b).

Nemoto, N., J. L. Schrag, and J. D. Ferry, "Infinite-dilution viscoelastic properties of poly(n-hexyl isocyanate)," Polym. J. **7**, 195–201 (1975).

Ookubo, N., M. Komatsubara, H. Nakajima, and Y. Wada, "Infinite-dilution viscoelastic properties of poly-γ-benzyl-l-glutamate in m-cresol," Biopolymers **15**, 929–947 (1976).

Pasquali, M., V. Shankar, and D. C. Morse, "Viscoelasticity of dilute solutions of semiflexible polymers," Phys. Rev. E **64**, 020802(R) (2001).

Pasquali, M. and D. C. Morse, "An efficient algorithm for metric correction forces in simulations of linear polymers with constrained bond lengths," J. Chem. Phys. **116**, 1834–1838 (2002).

Warren, T. C., J. L. Schrag, and J. D. Ferry, "Infinite-dilution viscoelastic properties of poly-γ-benzyl-l-glutamate in helicogenic solvents," Biopolymers **12**, 1905–1915 (1973).

Wiggins, C. H., D. Riveline, A. Ott, and R. E. Goldstein, "Trapping and wiggling: Elastohydrodynamics of driven microfilaments," Biophys. J. **74**, 1043–1060 (1998).